Master Thesis in Geosciences

Structural analysis of the Asterias Fault Complex in the SW Barents Sea

By

Mujtaba Mehmood Mongat

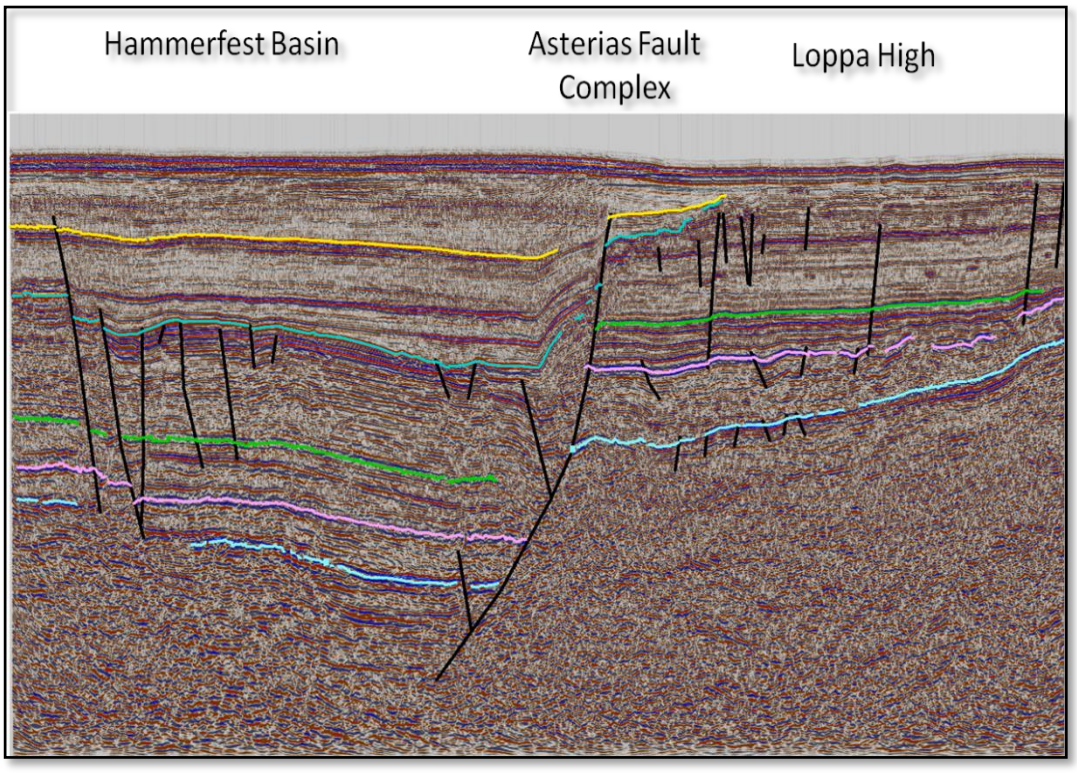

UNIVERSITY OF OSLO
FACULTY OF MATHEMATICS AND NATURAL SCIENCES

Structural analysis of the Asterias Fault Complex in the SW Barents Sea

Mujtaba Mehmood Mongat

Master Thesis in Geosciences

Discipline: Petroleum Geology and Geophysics

Department of Geosciences

Faculty of Mathematics and Natural Sciences

UNIVERSITY OF OSLO

June 30, 2011

Acknowledgements

I wish to extend my heartfelt appreciation to my supervisors, Prof. Jan Inge Faleide and Prof. R. H. Gabrielsen. Their encouragement and support throughout the length of this study is highly appreciated. I also owe special thanks to Dr. Michel Heeremans, co-supervisor, who helped in data handling and software support.

TGS-Nopec is acknowledged for making the seismic data avaliable

Sincere gratitude goes to my entire family for their continued support and love and having faith in me. Lastly, I would like to thank my friends for their care and for all those beautiful moments that I shared with them.

Contents

Acknowledgements ..... **i**
Abstract ..... **v**
1 Introduction **1**
2 Geological Framework **3**
2.1 Regional Setting 3
2.2 Main Geological Provinces 3
2.3 Geological Evolution 5
2.4 Main Structural Elements 6
2.5 Stratigraphy 8
2.6 Asterias Fault Complex 11
3 Seismic Interpretation and Results **13**
3.1 Data 13
3.2 Methodology and Procedure 13
3.3 Seismic Interpretation Procedure 15
3.4 Seismic to Well Tie 15
3.5 2D seismic interpretation 19
3.6 3D Seismic Interpretation 28
3.7 Description of Time Structure & Fault Maps 31
4 Discussion **39**
4.1 Model 1 – Tectonic inversion related to compressional stress system 40
4.2 Model 2 – Strike-Slip System 41
4.3 Model 3 – Extensional System "Roll-over Anticline associated with Listric Fault" 42
4.3.1 Fault plane profile of the master fault 42
4.3.2 Shape of rollover anticline 44
4.4 Structural Style of Asterias Fault Complex 46
4.4.1 The western segment of the Asterias Fault Complex 46
4.4.2 The Central Segment of Asterias Fault Complex 47
4.4.3 Eastern Segment of Asterias Fault Complex 48
4.5 Geological Evolution of the Asterias Fault Complex 48
4.5.1 Mid Carboniferous to Early Permian 48
4.5.2 Late Permian to Jurassic 49
4.5.3 Late –Middle Jurassic onset of rifting 51
4.5.4 Early Cretaceous–Subsidence 51

4.5.5 Tertiary – Recent..... 54
5 Conclusions..... 57
References..... 59

Abstract

Asterias Fault Complex is present in the SW Barnets Sea and is extensional in nature. This fault complex separates the Hammerfest Basin in south from the Loppa High in north

Variations in structural trend and frequency of deformation (associated synthetic and antithetic faults and related structures) warrant subdivision of fault complex from west to east as (i) the western segment (ii) the central segment and (iii) the eastern segment. The western segment is of particular interest because of related structural complexity and the associated antiformal feature. Previous models to explain deformational mechanism in western segment have been revisited, and a new model on the basis of new evidence on 3D seismic data is proposed. This model relates the deformation style in the western segment to extensional system comprising ramp-flat-ramp extensional faults.

Degree of deformation associated with the fault complex decreases from west to east and the main boundary fault changes geometry from ramp –flat- ramp in western segment to downward concave in central segment and finally ends up as planar normal fault. 2D/3D seismic reflection data does not support the idea of Carboniferous / Permian rifting while Late-Mid Jurassic to Early Cretaceous is well registered in the study area. Asterias Fault Complex has been assigned the age of Late-Mid Jurassic to Early Cretaceous.

1 Introduction

The Barents Sea area is bounded in the west by the eastern margin of the deep Atlantic Ocean and in the east by the Novaya Zemlya islands (Fig 1.1). The Franz Josef Land and Svalbard archipelago exist to the north of Barents Sea while the Norwegian and Russian coasts lie towards its south. It covers an area of about 1.3 million km^2 and has an average water depth of approximately 300 m; it is one of the largest areas of continental shelf on the globe (Dore 1995). It hosts the sedimentary strata from Paleozoic to Quaternary, which form a thickness of around 15 km. Western part of the Barents Sea, especially the Norwegian sector is well constrained as compared to the eastern (Russian) part because of better data availability and quality. Thereby, southwestern part of this region is relatively well known through number of studies based mainly on seismic data correlated to offshore boreholes and onshore outcrops (Gabrielsen et al., 1990; Faleide et al., 1993).

Present study encompasses the structural analysis of the Asterias Fault Complex in the south western Barents Sea (Fig 1.1) with the underlying purpose to comprehend the structural architecture of the fault complex and its evolution through time. The Asterias Fault Complex separates the Hammerfest Basin from the Loppa High in the SW Barents Sea and towards west it enjoins the Ringvassøy Loppa Fault Complex (Gabrielsen et al., 1990). During present study, major focus has been to comprehend the structural configuration of the western segment of the Asterias Fault Complex. Different possible mechanisms that may have resulted in present architecture of this area have been evaluated e.g., tectonic inversion related to compression, strike-slip related structuring and rollover anticline geometry.

During the course of study, 2D & 3D seismic data have been utilized for structural interpretation. Information from three wells (taken from NPD) have been used for well to seismic calibration. Schlumberger's Petrel G&G software has been employed for interpretation from start till end. The study is divided into following interconnected phases:

Phase 1: Seismic & well data loading (2D/3D data sets & 3 wells, checkshot surveys)

Phase 2: Interpretation of regional 2D seismic lines, seismic to well ties for stratigraphic calibration

Phase 3: Detailed interpretation of seismic data, structural analysis for estimating timing and style of faulting during which results are synthesized to understand the interplay of faulting, uplift/erosion and subsidence/deposition

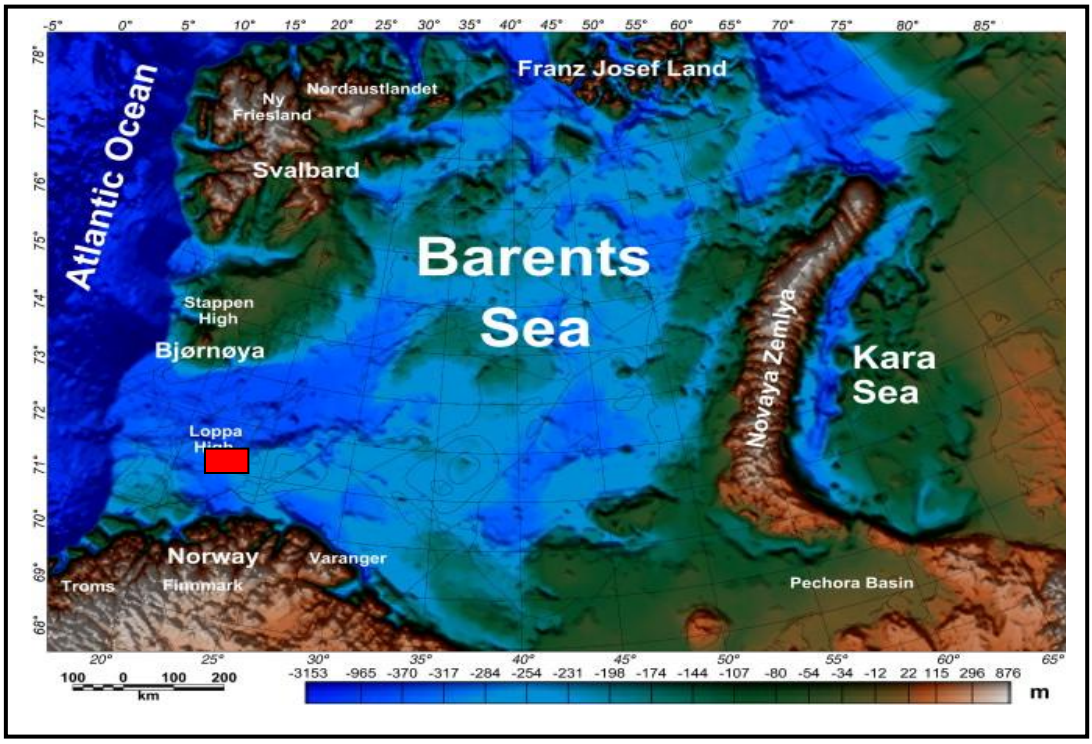

Fig. 1: Location map of the Barents Sea, showing the principal structural features and study area the southwestern (SW) Barents Sea (69°N–75°N and 13°E–30°E) (modified from Barrère et al 2008). Study area marked with red Colour.

2 Geological Framework

2.1 Regional Setting

The southwestern Barents Sea is characterized by some of the deepest sedimentary basins worldwide. These basins were formed as a result of several phases of regional tectonism within the North Atlantic-Arctic region during the continental separation of Eurasia and Greenland and accretion of oceanic crust in the Early Tertiary. During the crustal breakup, the southwestern Barents Sea was affected by focus of two structural mega-lineaments i.e. the North Atlantic rift zone (between the present Charlie Gibbs and Senja Fracture Zones) and a shear zone (the De Geer Line between Svalbard and Greenland) which continued into the Arctic Ocean along the North Greenland and Canadian continental margin (Faleide et al., 1993).

The Barents Sea is situated on top of an intracratonic setting. A passive shear margin, which initiated in the Paleocene, borders the oceanic Norwegian Sea in the west of this basin. The Hornsund Fault Zone in the north and the Senja Fracture Zone to the south are the two related major shear elements (Fig. 2.1); (Rønnevik et al., 1984**).** The west of 20°E forms a transitional region between the oceanic basin in the west and a stable craton to the east (Jackson et al., 1990).

2.2 Main Geological Provinces

The south-western Barents Sea is divided into three distinct regions (Gabrielsen et al., 1990; Faleide et al., 1993) (Fig. 2.1).

1. The Svalbard Platform, a stable platform since Late Paleozoic covered by relatively flat lying succession of Upper Paleozoic and Mesozoic, dominantly Triassic sediments.
2. The Basin Province, characterized by number of sub basins and highs with increasing structural relief westward between Svalbard Platform and Norwegian Coast.
3. The western margin, divided into three main segments (a) a southern sheared margin along the Senja Fracture Zone (SFZ); (b) a central rifted complex south-west of Bjørnøya

associated with volcanism (Vestbakken Volcanic Province); and (c) a northern, initially sheared and later rifted margin along the Hornsund Fault Zone (HFZ). The continent-ocean transition occurs over a narrow zone along the line of Early Tertiary breakup and the margin is overlain by a thick Upper Cenozoic sedimentary wedge.

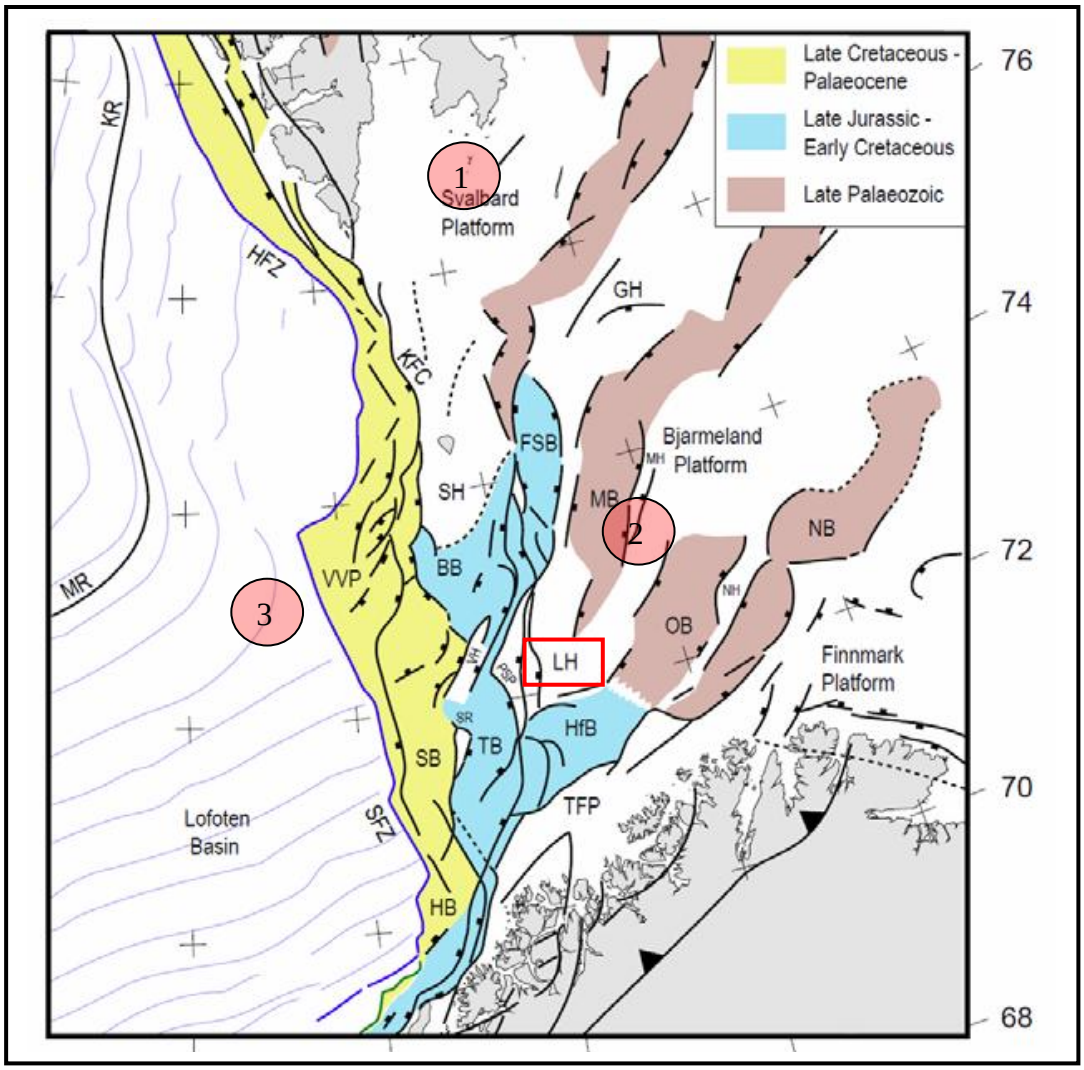

Figure 2.1: Main structural elements in the western Barents Sea and adjacent areas. Location of study area mark with red colour box (modified from Faleide et al., 2010). Numbers 1-3 shows location of three geological provinces.
BB = Bjørnøya Basin FSB = Fingerdjupet Sub-basin, GH = Gardarbanken High, HB = Harstad Basin, HfB = Hammerfest Basin, HFZ = Hornsund Fault Zone, KFC=Knølegga Fault Complex, KR = Knipovich Ridge, LH = Loppa High. MB = Maud Basin MH = Mercurius High, MR = Mohns Ridge, NB = Nordkapp Basin, NH = Nordsel High, OB = Ottar Basin, PSP = Polheim Sub-platform, SB = Sørvestsnaget Basin, SFZ = Senja Fracture Zone, SH = Stappen High, SR = Senja Ridge, TB = Tromsø Basin, TFP = Troms-Finnmark Platform, VH = Veslemøy High, VVP = Vestbakken Volcanic Province.

2.3 Geological Evolution

Three major episodes of rifting have been documented in the post- Caledonian history of the western Barents Sea, each influenced by several tectonic phases (Faleide et al., 1993)

1. Late Devonian?-Carboniferous.
2. Middle Jurassic-Early Cretaceous and
3. Early Tertiary.

Several interconnected extensional basins separated by fault-bounded highs were formed as a result of late Devonian (?)-Middle late Carboniferous rift phase (Gabrielsen et al., 1990). Tromøs, Bjørnøya, Nordkapp, Fingerdjupet, Maud and Ottar basins (Fig. 3) were formed during this time (Dengo & Røssland, 1992; Jensen & Sørensen, 1992; Bugge & Fanavoll, 1995; Breivik et al., 1995; Gudlaugsson et al., 1998). The western part of the Barents Sea has experienced more tectonic activities since Mesozoic. Its eastern and northeastern parts consist of relatively stable platform and have experienced less tectonism as compare to the western part throughout Mesozoic and Cenozoic era (Gabrielsen et al., 1990).

The Triassic to early Jurassic was a relatively quiet period because no major tectonic activity has been recorded in the region. Depositional patterns in the Nordkapp and Maud basin were influenced by salt tectonics during Triassic (Gabrielsen et al., 1990). In Middle-Late Jurassic, the southwestern Barents Sea underwent block faulting, with major faults trending along east and north-east directions and shales were deposited in restricted basins between tilted fault blocks (Faleide et al., 1993).

During Early Cretaceous, Barents Sea experienced extreme subsidence (documented in Tromsø and Bjørnøya basins) and major depocentres was developed in the Harstad, Tromsø and Bjørnøya basins (Breivik et al., 1998). This area also underwent local inversion along Ringvassøy–Loppa Fault Complex and its junction with Asterias Fault Complex, therefore structural development was complicated (Gabrielsen et al., 1990). Late Cretaceous was the period of reverse faulting and folding along with extensional faulting in some part of the region but extension may have prevailed on the regional scale (Gabrielsen et al., 1990).

Tromsø Basin continued to subside at slower rate due to salt movement during Tertiary (Faleide et al., 1993). Continental break up in the Norwegian-Greenland Sea is related to Paleocene-

Eocene transition. During this transition dextral sheared margin along with tensional component were developed on the western side of the Barents Sea (Faleide et al., 1993). During the Eocene and Oligocene periods, an event of peak folding and inversion occurred locally (Gabrielsen et al., 1990).

2.4 Main Structural Elements

The basins of SW Barents Sea were developed from oldest in the east and youngest in the west. The eastern part of SW Barents Sea holds three main basin of Late Paleozoic times associated with north east trend (Fig. 2.1); The Nordkapp Basin, Ottar Basin and Maud Basin. In Nordkapp Basin, it is difficult to mark the basin boundary exactly in some places because of poor penetration of seismic and halokinetic overprint. The Ottar Basin is situated in the north west of Nordkapp Basin. Two large salt domes are present within the Ottar Basin. The Maud Basin was developed in the north of Ottar Basin, where it is dominated by the Svalis Dome in south (Gudlaugsson et al., 1998).

Oceanic Basin

The Lofoten Basin developed as a result of Cenozoic sea floor spreading in the Norwegian – Greenland Sea. The Oceanic crust is approximately 4.5-6 km thick. The oceanic basement can be followed within a distance of about 10 km from continental boundary along the Senja Fracture Zone (Faleide et al., 1993).

Tertiary Marginal Basin

The Sørvestsnaget Basin is characterized by major tectonism during Tertiary breakup. The basin architecture was controlled by older structure underlying the intrabasinal highs (Senja Ridge, Veslemøy High, Stappen High) (Faleide et al., 1993).

Intrabasinal Highs

The intrabasinal highs in the south-western Barents Sea have been grouped together on the basis of similar structural and geophysical signature. These highs became positive feature within the Creataceous basin province during Late Cretaceous and Early Tertiary. The Senja Ridge separates the Tomsø Basin from the Sørvestsnaget Basin bounded by normal fault to the west.

(Faleide et al., 1993). The Veslemøy High, which was earlier considered as northern part of Senja Ridge (Gabrielsen., 1984) is now defined as a separate structural element (Gabrielsen et al., 1990). The Senja Ridge and Veslemøy High which developed as a positive structure element within the Cretaceous Basin province have been related to strike-slip faulting along the Bjørnøyrenna Fault Complex (Gabrielsen et al., 1990). The Stappen high was a part of a north-south trending elevated area in the western Barents Sea from late Paleozoic to Jurassic times (Faleide et al., 1993).

Cretaceous Basins

The Harstad, Tromsø and Børnøya basins experienced large scale Cretaceous subsidence and sedimentation. The Harstad Basin is in the south of Tromsø Basin. Salt diapirs exist along the axis of NNE trending Tromsø Basin (Faleide et al., 1993). This basin developed as a separate feature in Late Cretaceous when lateral movement took place along the Bjørnøyrenna Fault Complex (Gabrielsen et al., 1990). The Leirdjupet Fault Complex divides the Børnøya Basin into Fingerdjupet Sub- Basin which forms a deep western and shallow eastern part (Gabrielsen et al., 1990).

Cretaceous Boundary Faults

These eastern boundary faults are considered to be extensional in origin and developed mainly in Early Cretaceous. In the western side of the Loppa High, basement is present at shallow depth. The southern Troms-Finnmark Fault Complex and Bjørnøyrenna Fault Complex are dominating by Listric Faults. The Ringvassøy – Loppa Fault Complex comprises rotated fault blocks and cross cuts the Hammerfest Basin (Gabrielsen, 1984; Faleide et al., 1993).

Eastern Platform Region

The Eastern platform region comprises the Finnmark Platform, the Hammerfest Basin, eastern Bjørnøya Basin and Loppa High. These regions were affected by Jurassic rifting without large scale post-rift subsidence and have not been affected by Cretaceous tectonism (Faleide et al., 1993).

The Hammerfest Basin is characterized by deep, high angle faults detached above or within Permian sequence in the basin center. Hammerfest Basin was dominated by extensional faulting

and has experienced strike-slip deformation in Late Jurassic to Early Cretaceous (Berglund et al., 1986; Sund et al.,1986; Gaberielsen & Færseth, 1988; Faleide et al., 1993).

The Hammerfest Basin was formed during Late Devonian to Early Carboniferous (Rønnevik et al., 1984; Gaberielsen et al., 1990). This is in accordance with the separation of Hammerfest Basin from Finnmark Platform (Gaberielsen et al., 1990). The Hammerfest Basin bounds the Loppa High by the Asterias Fault Complex in the north (Gudlaugsson et al., 1998). It comprises an eastern platform and the western part is underlain by shallow basement. The western crest has been rejuvenated at least four times since Devonian but the present Loppa High is a result of Jurassic to Early Cretaceous and Late Cretaceous- Tertiary tectonism (Gabrielsen et al., 1990). The rotated fault blocks bounding the western crest of the Loppa High were formed in late Jurassic to Early Cretaceous, and were later reactivated (Faleide et al., 1993).

2.5 Stratigraphy

The seismic sequence stratigraphy of southwestern Barents Sea is calibrated by Faleide et al., (1993), based on the well data from the Hammerfest Basin and lithostratigraphic framework of Worsley et al., (1988). Middle Jurassic is the deepest sequence boundary in the southwestern Barents Sea, correlated to the Hammerfest Basin (Fig. 2.3). But there is also a possibility for the presence of Pre-Middle Jurassic succession similar to the surrounding areas (Faleide et al., 1993).

Pre-Middle Jurassic

Permo-Carboniferous rocks are mapable in the region and are expected to be similar to those of Svalbard, Bjørnøya and north-east Greenland. Triassic of the south-western Barents Sea has a considerable lateral thickness. The Lower-Middle Jurassic interval is dominated by sandstones which are present throughout the Hammerfest Basin, probably thickening towards the Tromsø Basin in the northwest. In the Hammerfest Basin Middle Jurassic sandstone is the main reservoir (Berglund et al., 1986; Faleide et al., 1993).

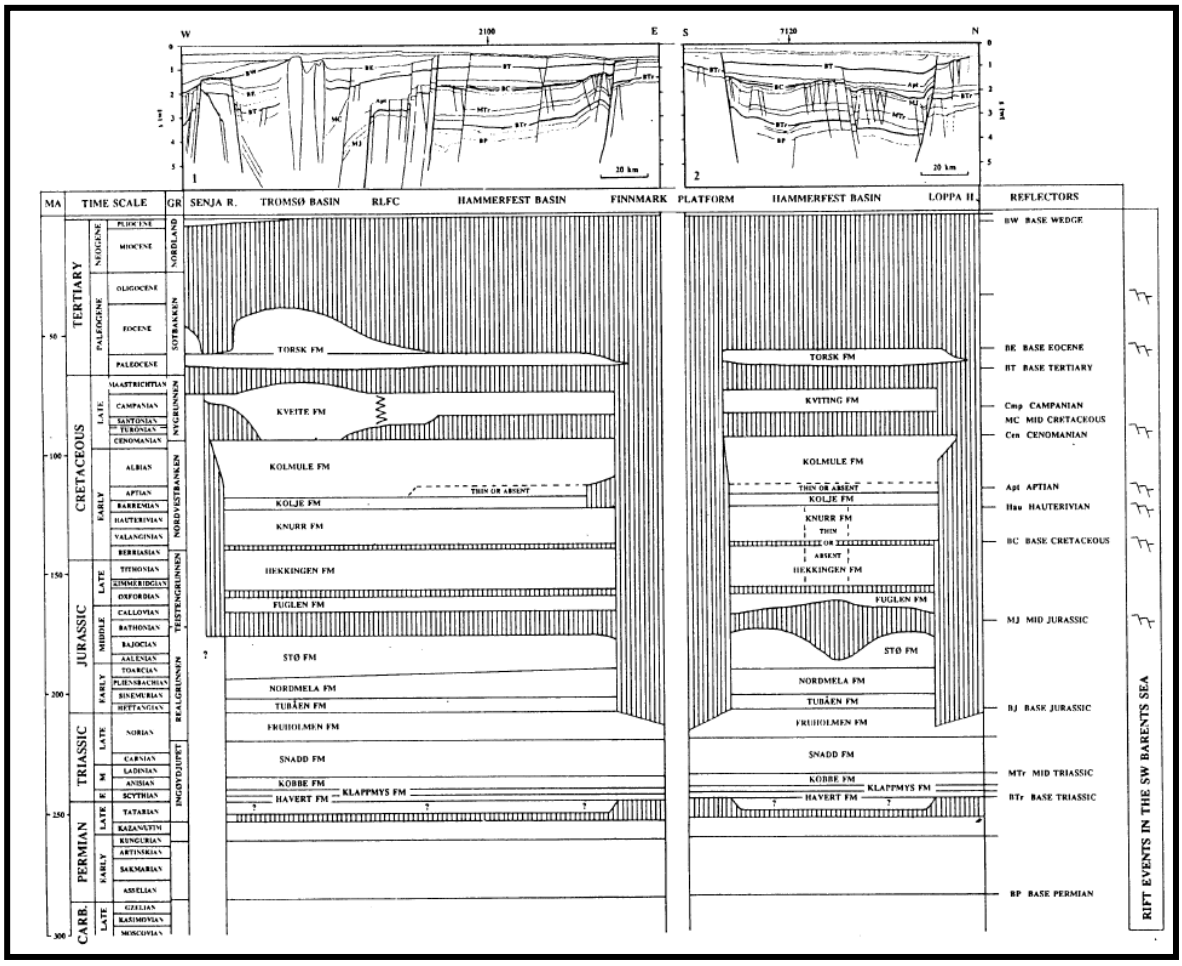

Fig 2.3: Stratigraphic summary: Main seismic sequences and reflectors related to lithostratigraphic framework of Worsley et al., (1988) and rift events in the south-western Barents Sea basin province. Chronostratigraphic chart based on two profiles (Figure from Faleide et al., 1993).

Middle-Upper Jurassic

The onset of rifting in the south-western Barents Sea is shown by MJ reflector in Figure 2.3 There is a considerable variation in the thickness of the Teistengrunnen Group. This group thins out towards the structural high in the central Hammerfest Basin and the thickness increases towards basin boundary fault to the north, south and west (Faleide et al., 1993) (Fig. 2.3).

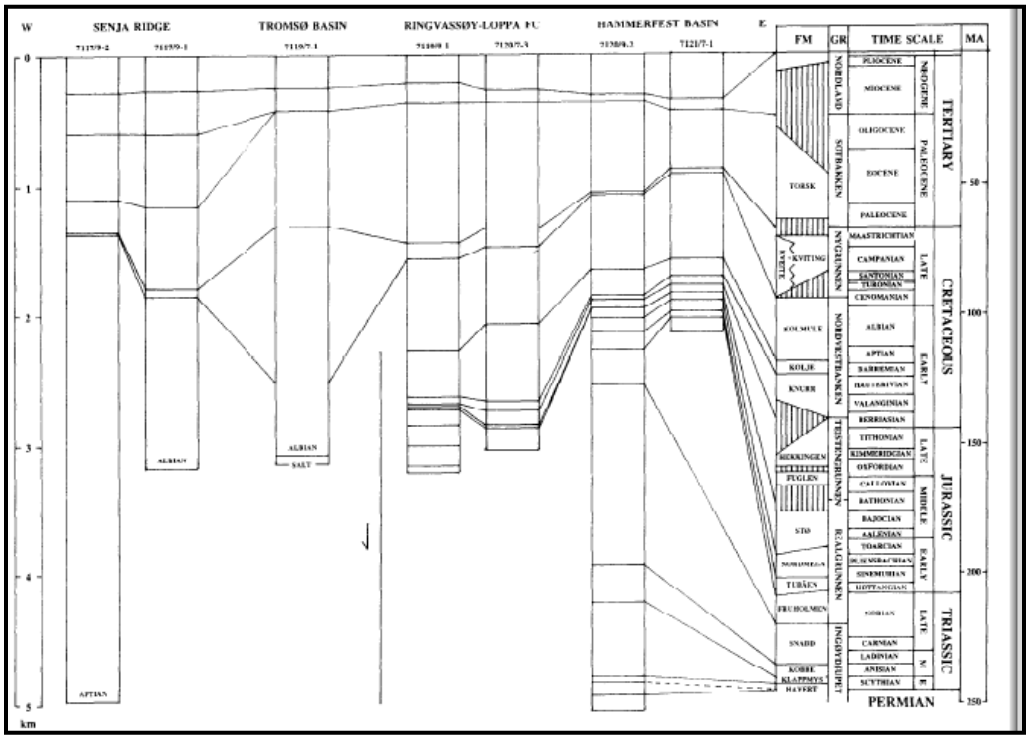

Figure 2.4: Well correlation along west-east transect from Senja Ridge to the Hammerfest Basin. Location of wells is shown in Figure 4 (from Faleide et al., 1993).

Lower Cretaceous

The Nordvestbanken Group consists of three formations i.e. Knurr Fm, Kolje Fm and Kolmule Fm. The Nordvestbanken Group gets thick towards the Ringvassøy-Loppa Fault Complex (Fig. 2.4) and to the north before onlapping against the Loppa High and to the south against the Finnmark Platform. There are certain stratigraphic horizons which are thin in Hammerfest Basin but get thicker towards the Tromsø Basin (Faleide et al., 1993).

Upper Cretaceous

It has been seen that in the Trømsø Basin, the Nygrunnen Group varies in thickness (Fig. 2.3 & 2.4). A shale succession of 1200 m was drilled in the Tromsø Basin while seismic data show that the sequence reaches 2000-3000 m in rim synclines within the central basin (Faleide et al., 1993). A thin Upper Cretaceous sequence is observed in the wells on the Senja Ridge (Fig. 2.4), indicating Late Cretaceous structuring and considerable salt-related subsidence in the Trømsø and Sørvestsnaget basins. The Upper Cretaceous interval is difficult to resolve on seismics due to

the thinning and the group in the Campanian times thins from 250 m to less than 50 m eastwards in the Hammerfest Basin (Worsley et al., 1988).

Palaeogene

The Sotbakken Group overlies unconformably on the Nygrunnen Group and this depositional break at the Cretaceous-Tertiary transition (Maastrichtian-Danian) is present throughout the south-western Barents Sea (Faleide et al., 1993; Worsley et al., 1988). In the central and eastern parts of the Hammerfest Basin the interval from Late Palaeocene (Thanetian) to Early/Middle Eocene (Ypresiani Lutetian) age is preserved (Worsley et al., 1988).

Neogene-Quaternary

There is an unconformable contact between Neogene-Quaternary Nordland Group and Palaeogene-Mesozoic rocks getting thick in the huge sedimentary wedge towards the margin (Faleide et al., 1993) (Fig.2.4). The age of the sediments in the Hammerfest Basin is Late Pliocene to Pleistocene/Holocene Basin (Worsley et al., 1988). The major part of this wedge at the Senja Ridge is considered to be of Late Pliocene/Pleistocene and is of glacial origin. This implies that the glacial sediments in the Hammerfcst Basin are 100-200m thick, their thickness increase to 700 m at the Senja Ridge (Fig. 2.4) and further increases to about 4000 m in the Lofoten Basin (Faleide et al., 1993 & 1996).

2.6 Asterias Fault Complex

The Asterias Fault Complex is located between $71^{o}50'N$, 20^{0} E and $72^{o}20'N$, 24^{o} E. The E-W (Fig. 2.1) trending Asterias Fault Complex separates Hammerfest Basin from Loppa High and is believed to be extensional in origin (Gabrielsen et al., 1990) also known as Southern Loppa High Fault System (Gabrielsen et al., 1984; Gabrielsen., 1984; Faleide et al., 1984; Berglund et al., 1986). The Asterias Fault Complex is a basement involved first or second order structure which initiated between Triassic to Jurassic (Gabrielsen et al., 1984). This fault complex is associated with very complex pattern of southerly and northerly dipping faults (Berglund et al., 1986).

The western segment (west of 21°15'E) of Asterias Fault Complex shows evidence of inversion, half flower and local doming. Its northeasterly segment (northeast of 22°E) developed as a flexure underlain by deep extensional fault (Berglund et al., 1986; Gabrielsen et al., 1990).

The thickness of upper Triassic increases towards Loppa High across the Asterias Fault Complex, indicating that the Asterias Fault Complex was active at that time probably as an inverse structure and Loppa High area was depocentre(Gabrielsen et al., 1990).. Onlaps of Aptian- Albian reflectors on the eroded part of the Loppa High indicate strong uplift took place during Early Cretaceous along the fault complex (Gabrielsen et al., 1990). Asterias Fault Complex is believed to be extentional in origin. (Gabrielsen, 1984; Gabrielsen et al., 1990). However it is suggested that this fault zone had experienced compressional strike-slip movement and this structure collapsed into normal fault at the beginning of Cretaceous time (Berglund et al., 1986).

3 Seismic Interpretation and Results

3.1 Data

The data set comprises of 2D reflection seismic lines, a 3D Survey and well data. Data coverage along the Asterias Fault Complex is particularly good that includes some part of the Loppa High and the Hammerfest Basin.

2D seismic lines are taken from several seismic surveys (Fig. 3.1). 2D seismic lines selected for this study follows the structural trend of Asterias Fault Complex. A 3D survey is used for more detailed study of particularly significant part of the study area (western part) along with the 2D seismic lines (Fig. 3.1). Wells 7121/1-1, 7120/2-1 and 7120/9-2 were used for stratigraphic calibration. Lithostratigraphic information of these wells is taken from NPD (Table 3.1). The well 7120/2-1 is located on the Loppa High and has penetrated the basement at 3471 m depth. The second well 7121/1-1 is drilled on the Loppa High with the oldest penetrated Ørn Formation at 3990 m depth. The third well 7120/9-2 is located in the Hammerfest Basin, drilled down to Røye Formation at 4956 m depth (www.npd.no). The key horizons have been defined using the well tops from these wells. Wells have been used on either side of the Asterias Fault Complex; therefore stratigraphic markers on both sides of the fault complex will be controlled by well information.

3.2 Methodology and Procedure

Petrel 2009 was used to interpret the seismic reflection data. Petrel is"Windows-based Software" developed by Schlumberger, used for seismic interpretation, well correlation, reservoir simulation models, volumetric calculations and various maps generation etc (ww.slb.com). The following work flow is followed during seismic interpretation.

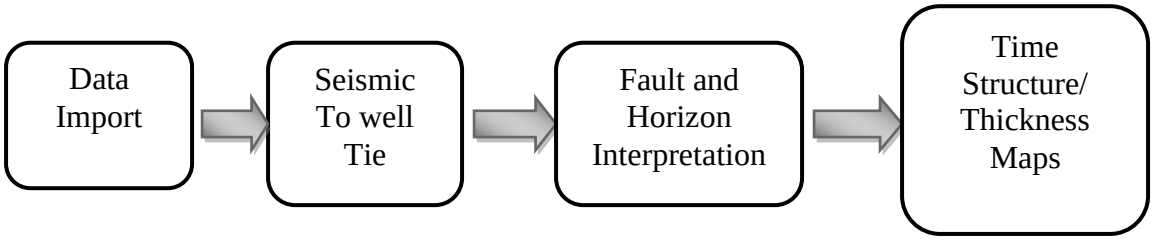

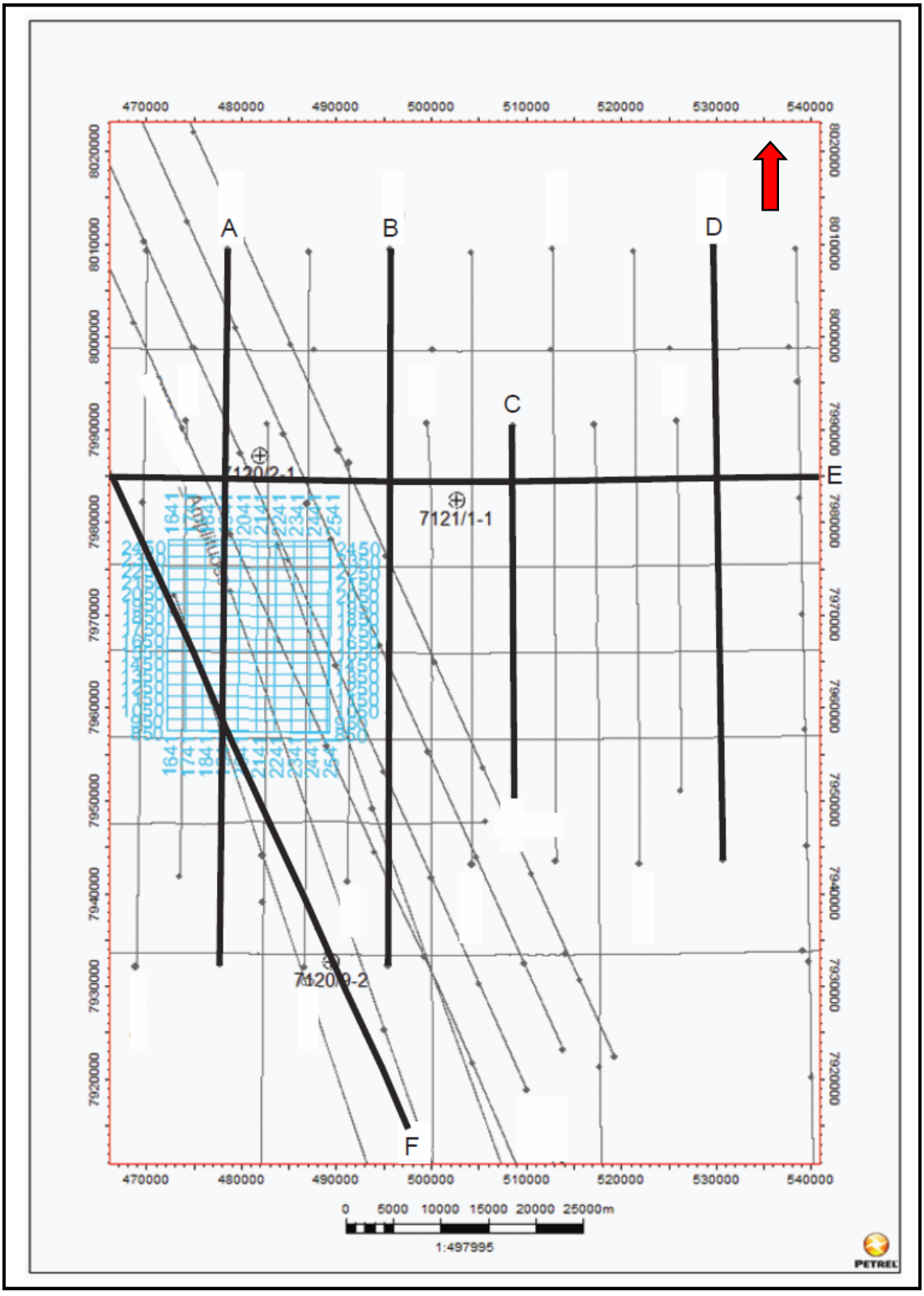

Fig. 3.1: Base map of the study area showing location of 2D seismic lines, 3D seismic survey NH9605 and well locations.

Lithostratigraphic Unit	7120/9-2 Top Depth (m)	7121/1-1 Top Depth (m)	7120/2-1 Top Depth (m)
Kviting Fm	1072	-	-
Hekkingen Fm	1906	-	-
Kapp Toscana Gp	1971	698	613
Snadd Fm	2552	792	613
Sassendalen Gp	3962	2210	1933
Kobbe Fm	3962	2210	1933
Tempelfjorden Gp	4844	2993	-
Røye Fm	4956	2993	-
Ugle Fm	-	-	2221

Table 3.1: Well tops used in the study (www.npd.no).

3.3 Seismic Interpretation Procedure

Seismic Interpretation exercise was carried out firstly on hard copy print of composite 2D seismic line 205230, covering area from the Loppa High in north to the Tromsø-Finnmark Platform in the south and running through the entire Hammerfest Basin.

After getting used to of the structural elements present within the study area, 2D seismic interpretation was proceeded on Petrel 2009. Well data consisting of well tops and checkshot surveys are imported in ASCII format. Seismic to well tie for the stratigraphic calibration was done using wells' checkshot survey (Section 3.4). Once stratigraphic calibration is done various reflection and fault interpretation was carried out. It was followed then by 3D seismic interpretation; however, 3D seismic data was limited to the western portion of the study area and covers the Asterias Fault Complex only (limited coverage on the Loppa High and the Hammerfest Basin). Major interpretation was carried out on 2D seismic lines of various surveys (Fig. 3.1).

3.4 Seismic to Well Tie

In this study five reflections are selected to map out the Asterias Fault Complex. The reflectors with their colour codes are shown in the Table 3.2. Horizons are depth controlled with the help of well tops data.

Reflector	Formation	Age (Ma)	Colour
Intra Carboniferous	Ugle Fm	318.1	
Intra Permian	Røye Fm	265.8	
Intra Triassic	Kobbe Fm	228	
Base Cretaceous	Hekkingen Fm	145.5	
Base Tertiary	Kviting Fm	70	

Table 3.2: Colour codes of interpreted reflector in the study area.

As mentioned earlier, well data from three wells was used for well to seismic correlation. The well 7120/2-1 and 7121/1-1 are about 2 kms away from the 2D seismic line E. Well 7120/9-2 is located in the Hammerfest Basin, on the seismic line F. Each of these wells is tied with the respective seismic lines. Well ties from different wells are shown in the (Fig. 3.2 and Fig. 3.3).

Intra Carboniferous is the lowermost reflection interpreted in the study area (Fig. 3.2). Top Ugle Formation is interpreted as Intra Carboniferous between 2250-4500 milliseconds TWT approximately. It is characterized by strong reflection, moderate to low frequency, medium amplitude with chaotic reflections. Well control is available on the Loppa High whereas 2D seismic line from the most eastern side is used for correlation of Intra Carboniferous into the Hammerfest basin.

Intra Permian has been picked within Røye formation between 2400- 4000 milliseconds approximately (Fig. 3.2). Intra Permian is a strong reflection with medium-high amplitude and moderate to low frequency. There has been considerable complexity in correlating it within the fault complex however it is easily followed through-out the Hammerfest Basin and Loppa High.

Top of Kobbe Formation has been interpreted as Intra Triassic between 1750-3600 milliseconds TWT, approximately (Fig3.3). On the Loppa High, the Intra Triassic reflection is characterized by high-moderate frequency, medium to low amplitude and good continuity. Particularly, its amplitude decreases considerably in the Hammerfest Basin. Pattern of Intra Triassic reflection becomes discontinuous and chaotic within the uplifted structure at the western extremity of the Asterias Fault Complex.

Base Cretaceous is defined by Top Hekkingen Formation that has been interpreted as strong positive reflection between 2500- 1000 ms TWT. (Fig3.3). It is characterized by high frequency

and high amplitude both on 2D and 3D seismic lines and easily interpreted throughout the Hammerfest Basin

Base Tertiary is the shallowest horizon that has been interpreted between 1450-700 milliseconds, corresponds to top of Kevite Formation as reflection (Fig. 3.3). The amplitude varies from medium to high and characterized by high frequency.

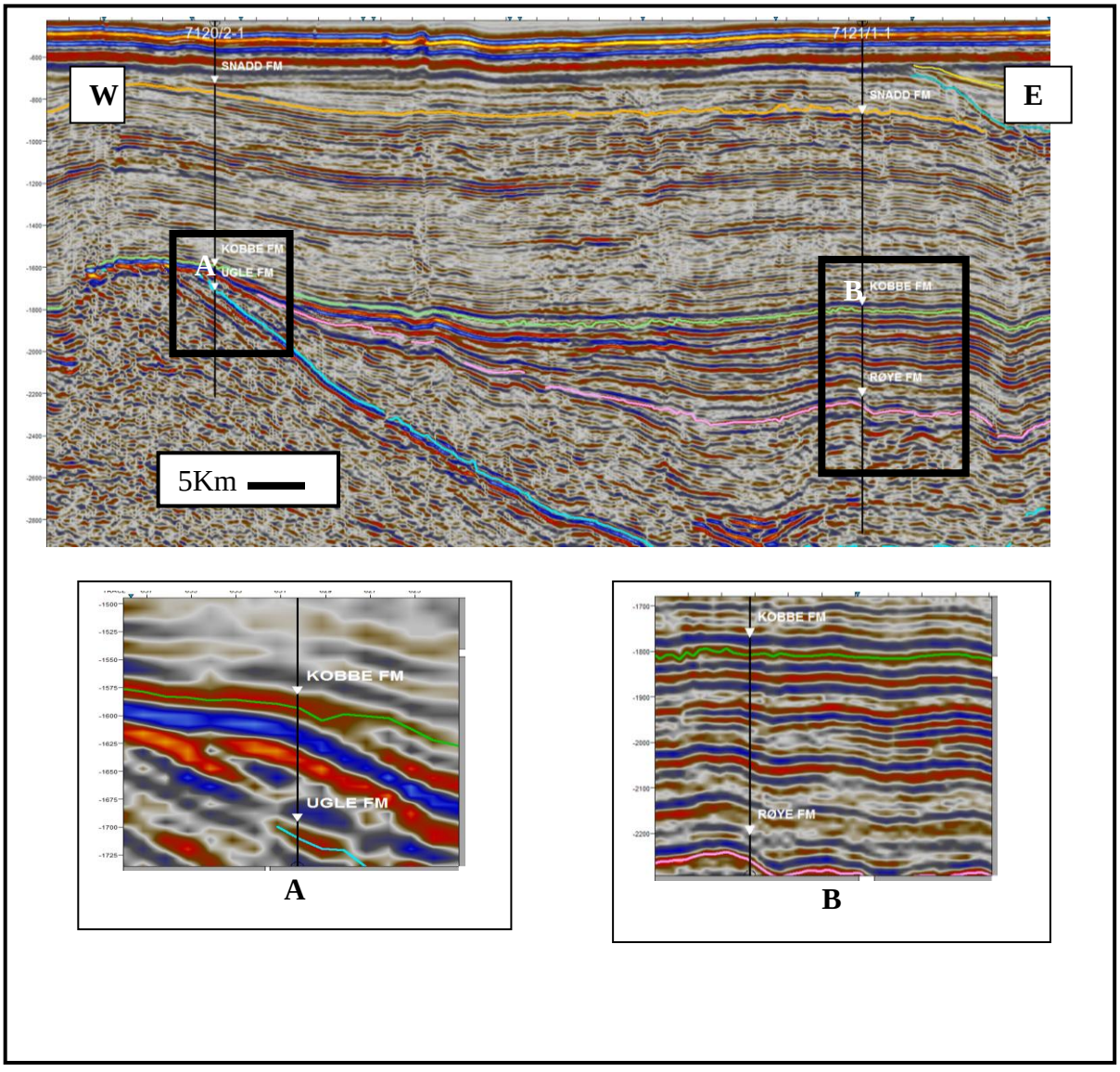

Fig. 3.2: Seismic to well calibration for wells 7120/2-1 and 7121/1-1. Figs. 3.2 A & B show closer view of calibration with well data (see the colour code for reflection in table 3.2). See Fig. 3.1 for location (Line E).

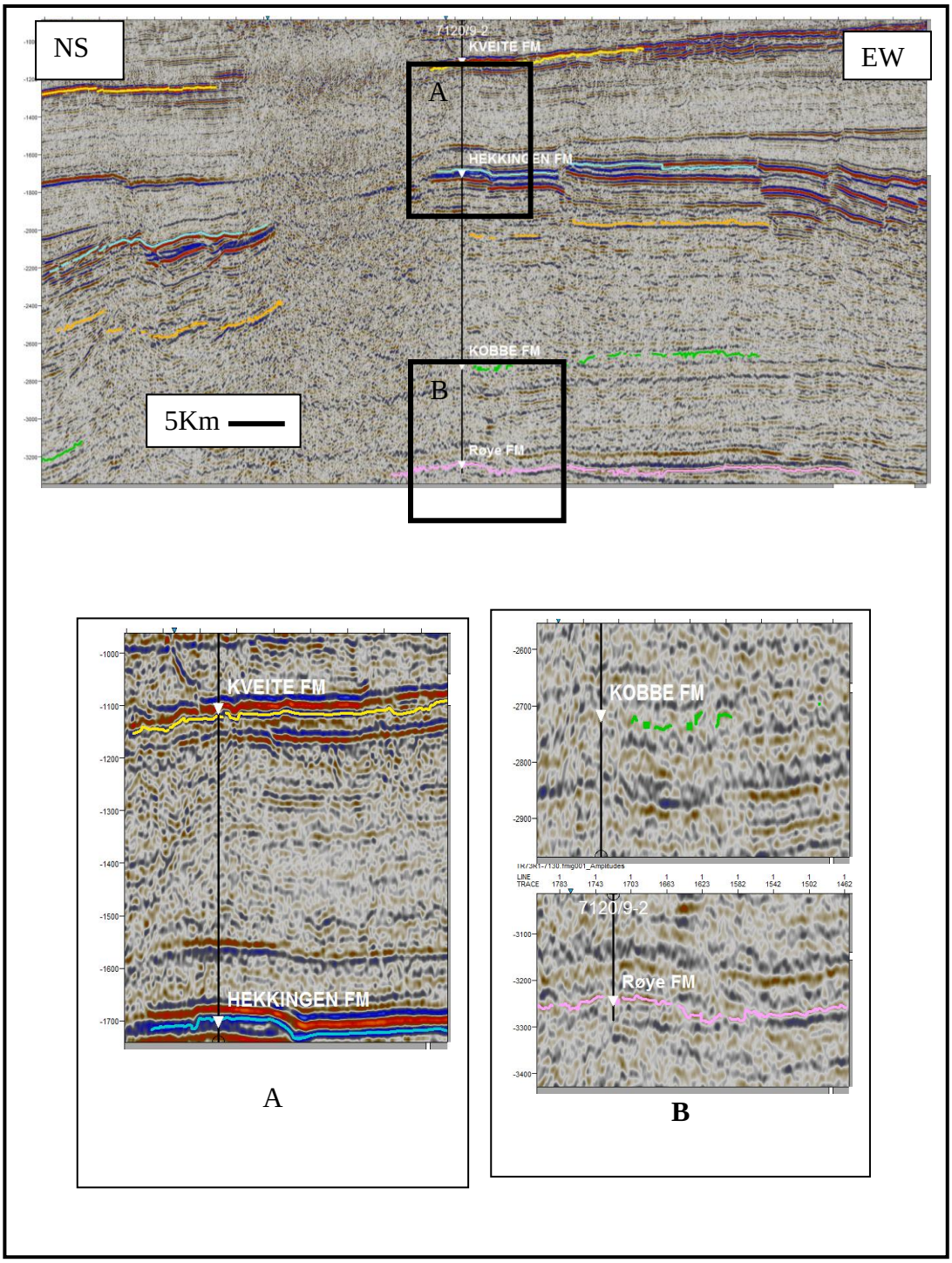

Fig. 3.3: Shows the well tie to 7120/9-2 on the Line F (see the colour code for reflection in table 3.2) see fig 3.1 for location..

3.5 2D seismic interpretation

The E-W trending Asterias Fault Complex separates the Hammerfest Basin from the Loppa High and is believed to be extensional in origin (Gabrielsen et al., 1990). This fault complex is a basement involved first or second order structure which initiated between Triassic to Jurassic (Gabrielsen et al., 1984). The Asterias Fault Complex is associated with very complex pattern of southerly and northerly dipping faults (Berglund et al., 1986). The western segment defines the junction of the Asterias Fault Complex with the Ringvassøy-Loppa Fault Complex (Gabrielsen et al., 1990). Its northeasterly segment (northeast of 22^{o}E) developed as a flexure underlain by deep extentional fault (Berglund et al., 1986; Gabrielsen et al., 1990).

2D seismic interpretation is aimed at describing all structural elements and their sub-elements present within the study area. Therefore, 2D seismic dip lines were selected first as truly representing the cross-sectional view, for better understanding of the interplay of structure and sedimentation. Four (4) key 2D seismic dip lines (A-D, Fig 3.1), are termed as key profiles and explained later in this chapter as these proflies best describe the change in structural trend and geometry of the Asterias Fault Complex. Predominantly, E-W trending Asterias Fault Complex changes strike from west to the east and hence, has been divided into three separate segments, a western, a central and an eastern segment on the basis of geometry and structural trend, which will be dealt with in chapter 4 (Fig. 3.4 & Fig. 3.5).

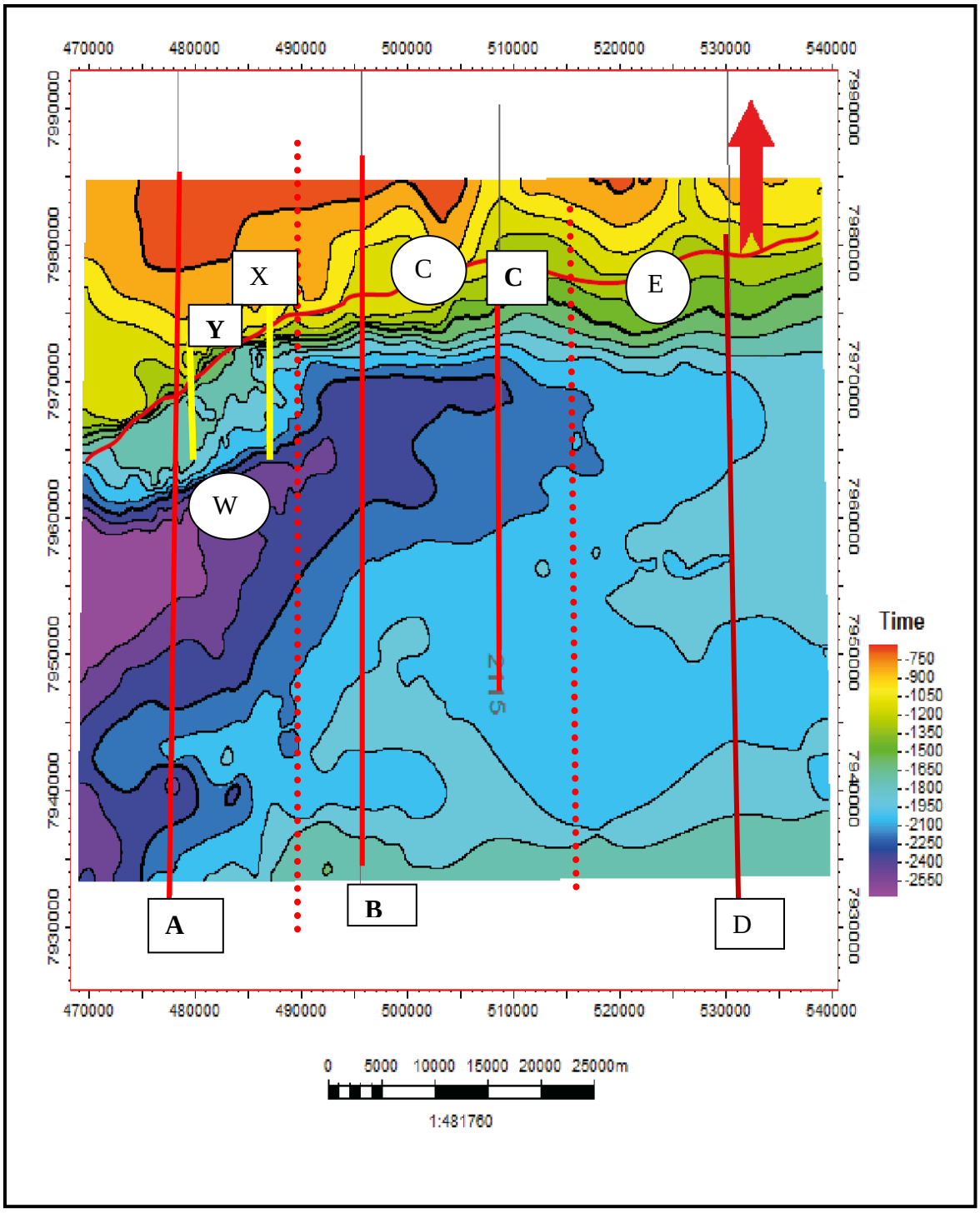

Fig. 3.4: Time Structure map at Base Cretaceous level of study area. Dotted lines showing three segments W (western) C (central) and E (eastern) while continuous lines showing position of seismic lines . E-W red line showing limit of Lower Cretaceous

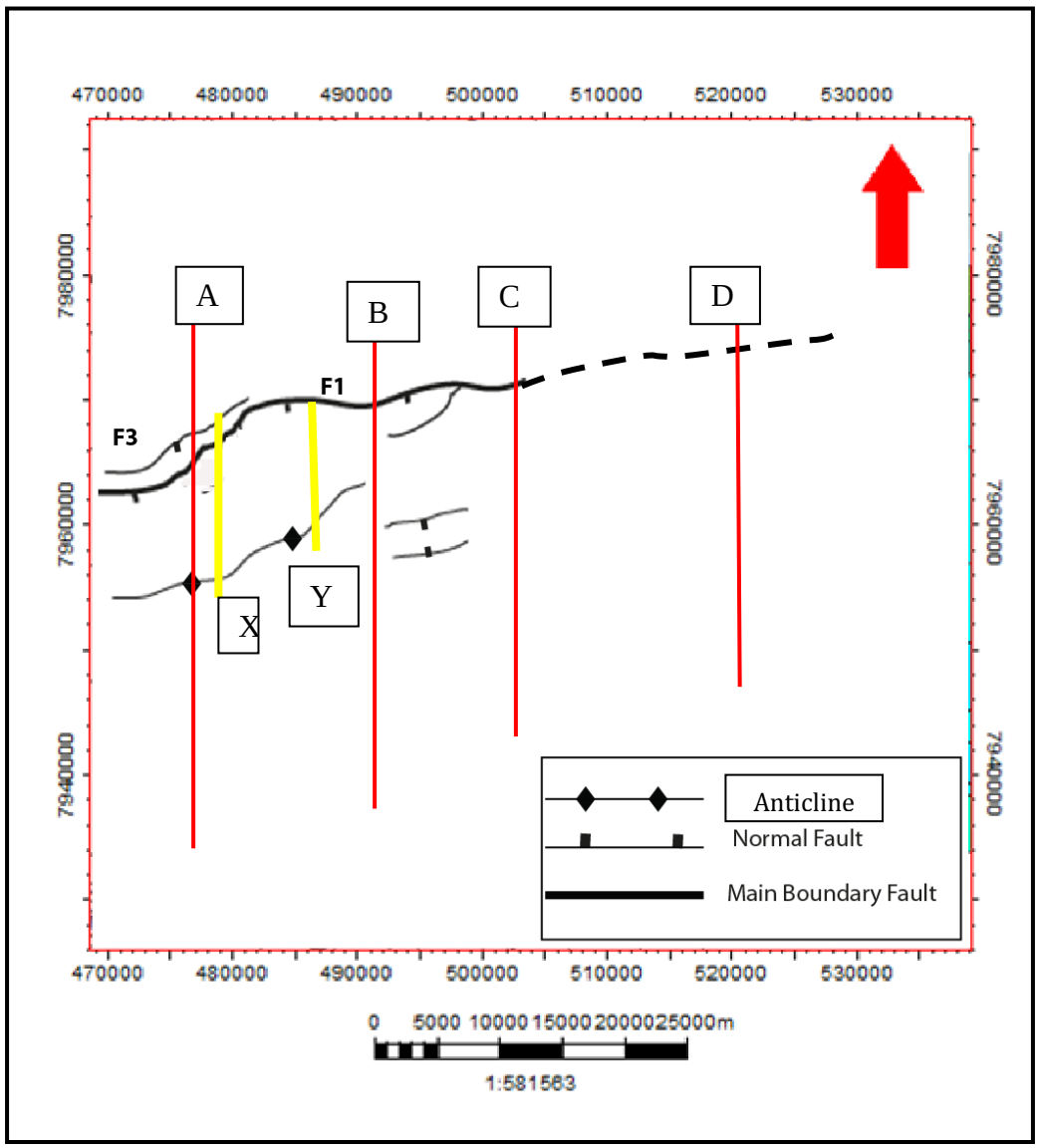

Fig. 3.5: Fault map showing the trend of Asterias Fault Complex at Base Cretaceous level, Black dotted line show presence of deep rooted fault at this location.

2D Seismic Line A

2D seismic line A is north-south oriented and located in the western part of the study area (Fig. 3.4, Fig. 3.5). Asterias Fault Complex in this profile is encompassing two normal fault strands (Fig. 3.6). The northern main boundary fault F1 shows listric geometry, (Fig. 3.6) a general south dip that varies with depth and follows a general ENE-WSW trend (Fig. 3.5). The main boundary fault cuts stratigraphic succession from Early Tertiary to the Permian while it seems to have

flattened in Permian strata making it a detachment horizon (Fig 3.6A). The other master fault (F2) is planar in nature and dips to the south trending ENE-WSW (Fig 3.5).

Majority of the faults encountered in the hanging wall (the Hammerfest Basin) are synthetic to the F1 (main boundary fault) while synthetic faults to the main boundary fault have also been observed farther towards basin (Fig. 3.6). Three synthetic faults of main boundary fault dips to the south (Fig. 3.6A). These planar faults exhibit normal geometry and have penetrated the strata from Triassic to Late Cretaceous (Fig. 3.6A). North-dipping normal faults that cut succession from the Intra Carboniferous to Intra Triassic form a typical half graben where reflections are tilted towards the main boundary fault (Fig. 3.6). Similarly, a younger south dipping normal fault that cuts section from Late Jurassic-Early Cretaceous has been involved in the formation of a minor half graben, which forms a small sedimentary wedge that decreases in thickness towards south and the reflections gently dip towards north (Fig. 3.6). Narrow horst and graben features are also associated with the Late Jurassic-Early Cretaceous strata (Fig. 3.6).

Frequency of faulting decreases however, towards the footwall (the Loppa High), where only minor faults in Late Triassic sequence are observed (Fig. 3.6). On the Loppa High, the majority of the faults are synthetic to the south dipping main boundary fault. A paleo-high / ridge is also identified on the footwall at Intra Carboniferous level (Fig. 3.6). Cretaceous strata has not been observed on the Loppa High suggesting non deposition or erosion following uplift.

In the Hammerfest Basin, main boundary fault F1 accompanied by antithetic and synthetic normal faults results in the formation of an antiformal feature (Fig. 3.6A). In this profile stratigraphic sequence from Triassic to Late Cretaceous has been influenced by this feature (Fig. 3.6B). Towards the main Boundary Fault F1 decrease in thickness of strata above Base Cretaceous reflection is observed (Fig. 3.6C). Evidence from the profile suggests that Late Jurassic – Early Cretaceous was the period of syn-rift deposition.

All interpreted reflections from Hammerfest Basin dip gently towards north (Fig. 3.6). However, Base Cretaceous & Intra Triassic reflections dip south and become shallow within Asterias Fault Complex (Fig. 3.6A). It is however, noteworthy that dips of strata within the fault complex are structurally controlled. Northerly dipping reflections before shallowing towards Asterias Fault Complex indicate subsidence of the Hammerfest Basin.

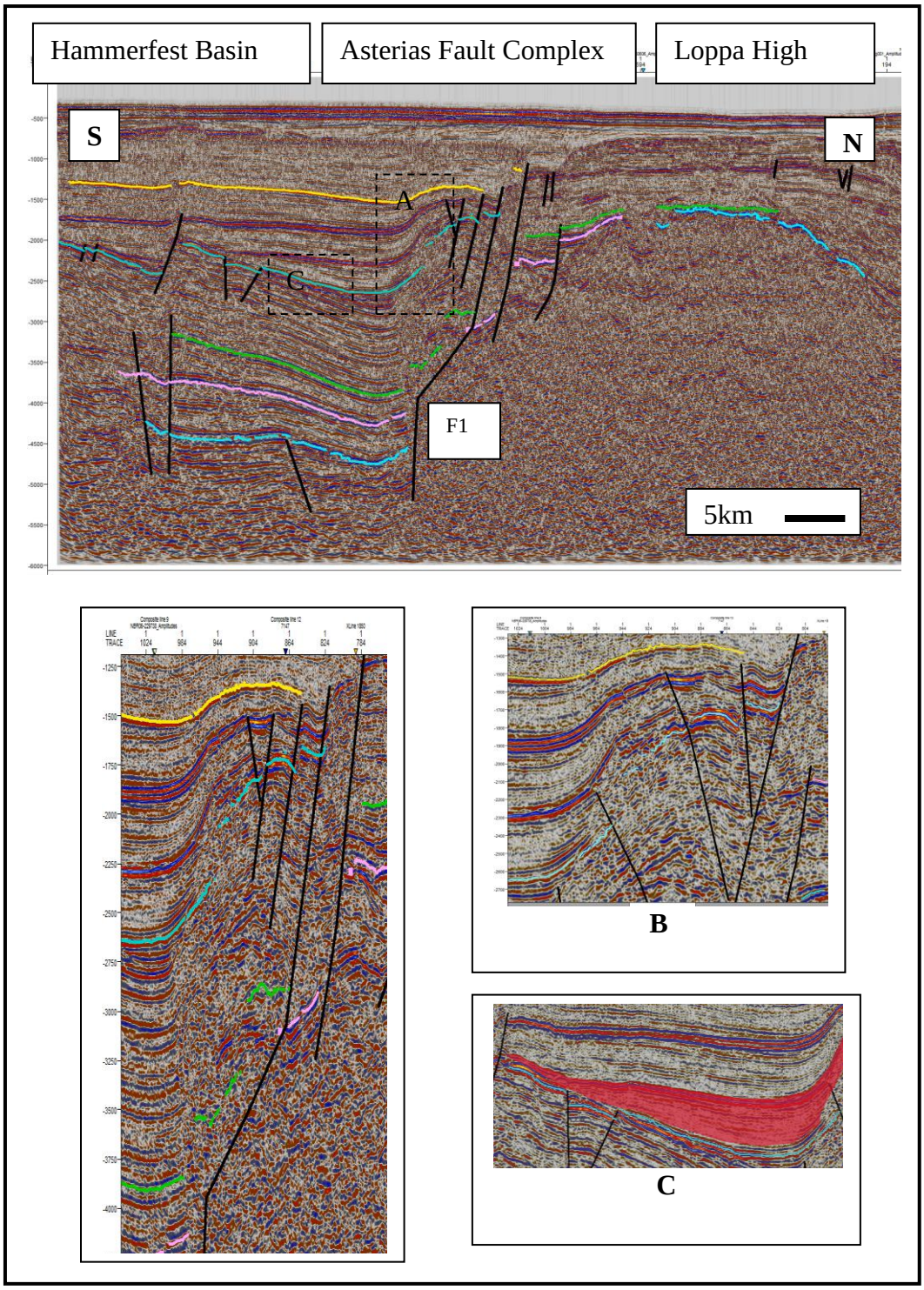

Fig. 3.6: Interpreted 2D Seismic Line A (see Fig 3.1, 3.4 & 3.5 for location), Fig 3.6A: Close up of Asterias Fault Complex with a normal main boundary fault. Fig 3.6 B: Close up view of anticlinal feature. Fig 3.2C: Thinning of Lower Cretaceous strata in hanging wall within Asterias Fault Complex shown in red highlighted area (see the colour code for reflections in Table 3.2).

2D Seismic Line B

2D seismic line B (Fig. 3.7) is north-south oriented and located in the central part of the study area (Fig. 3.4, Fig 3.5). The main boundary fault at Intra-Permian level appears to dip steeply, while it further steepens towards younger stratigraphic sequences and is generally showing an EW trend in map view (Fig. 3.4). This downward concave fault (F1) has a vertical throw of c. 1400 ms TWT with reference to the Intra Triassic reflection and is rooted in the basement (Fig. 3.7), indicating that it is a first or second order structure, in the terminology of Gabrielsen. (1984). This fault terminates in the Tertiary sequence (Fig. 3.7).

In the hanging wall, majority of the faults encountered are steeply dipping and are antithetic to the main boundary fault (Fig. 3.7). Two antithetic splays to the main boundary fault are observed in this profile which is dipping towards north and exhibits normal geometry. These antithetic splays cut stratigraphic section from Late Triassic to Late Jurassic (Fig. 3.7). Towards south, minor graben has been observed in the Jurassic strata, while a narrow horst and graben have also been observed further southward within Permian strata (Fig. 3.7).

On the Loppa High, most of the faults are steeply dipping, synthetic to the south dipping main boundary fault. Majority of these synthetic faults remain within Late Triassic sequence while few of them cut strata as old as Permian (Fig. 3.7). Early Cretaceous strata onlaps onto the Loppa High, indicating strong uplift during Early Cretaceous (Fig. 3.7A) and a general decrease in thickness of strata above Base Cretaceous reflection within fault complex is observed (Fig. 3.7B).

2D Seismic Line C

This N-S oriented line has been selected from the eastern most part of the central segment (Fig. 3.4, Fig. 3.5). The main boundary fault F1 it is dipping to the south (Fig. 3.8) and shows a general ENE-WSW trend (Fig. 3.5). This planar fault cuts stratigraphic section from the Carboniferous to the Early Cretaceous. The main boundary fault F1 has a vertical throw of c. 800 ms TWT with reference to the Intra Triassic reflection and shows normal geometry (Fig. 3.8). Stratigraphic thicknesses across the Asterias Fault Complex are similar except for the Jurassic level which shows decreased thickness on the footwall because of uplift and erosion.

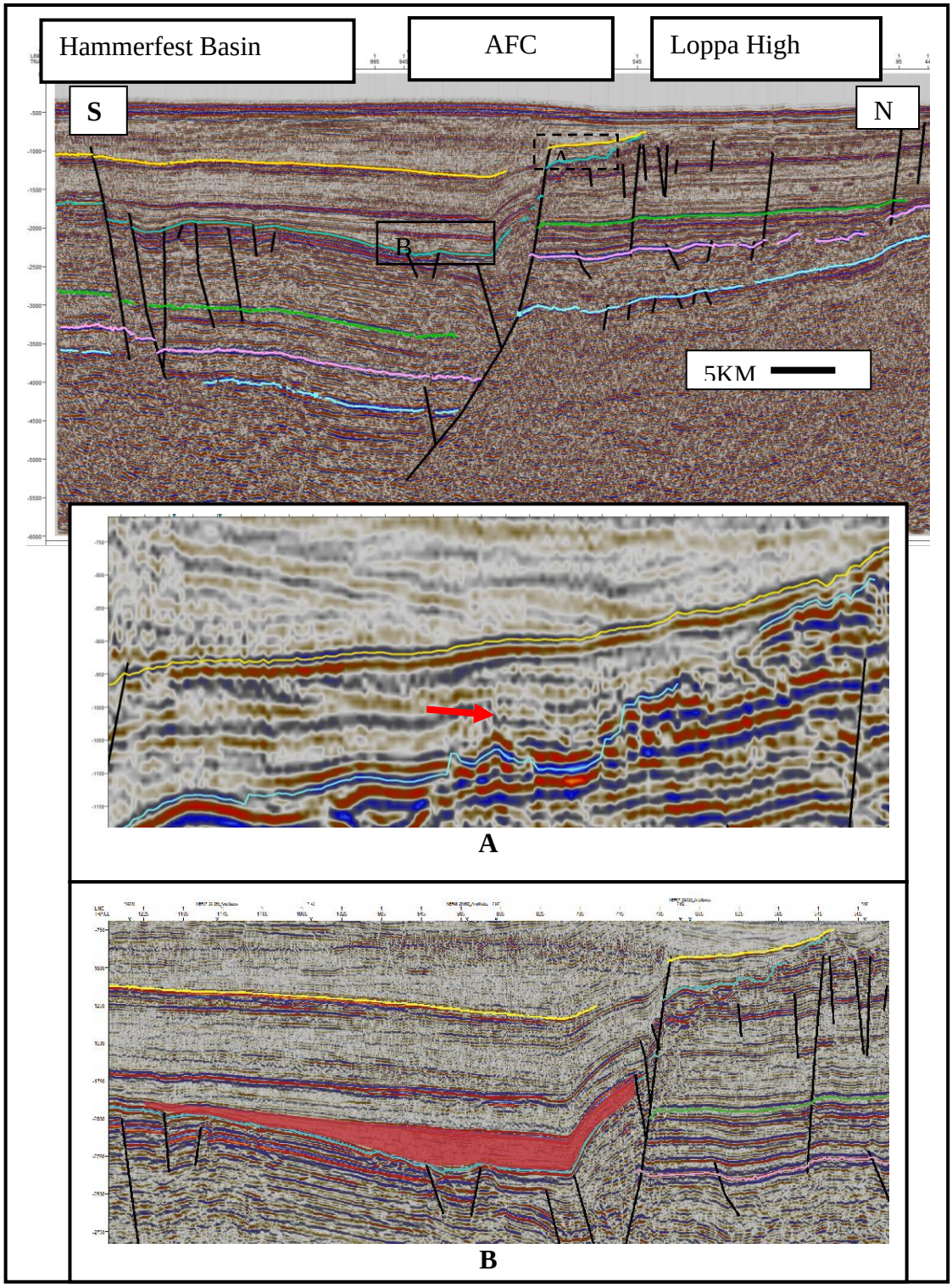

Fig. 3.7: Interpreted 2D Seismic Line B (see Fig 3.1, 3.4 &3.5 for location). Fig. 3.7A: Red arrow showing onlapping of Cretaceous strata onto eroded Loppa High. Fig.3.7B: Red highlighted area showing thinning of Lower Cretaceous in hanging wall block of Asterias Fault Complex (see the colour code for reflections in Table 3.2).

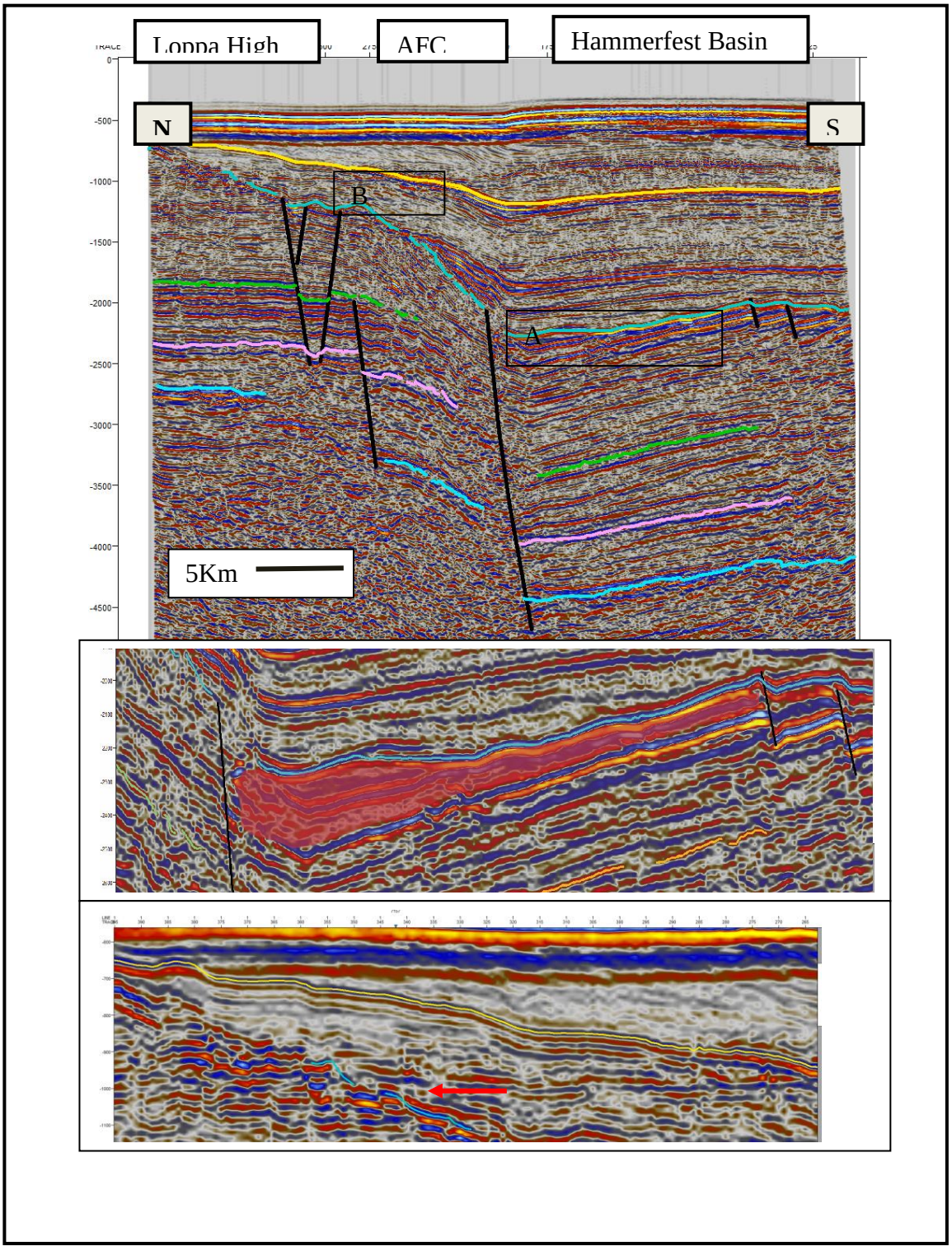

Fig. 3.8: Interpreted 2D seismic Line C (see figure 3.1,3.4 3.5 for location). Fig 3.8 A: Red highlighted area showing sedimentary wedge of Jurassic – Creataceous strata. Fig 3.8B: Red arrow pointing Cretaceous strata onlapping onto the Loppa High (see the colour code for reflections in Table 3.2).

In the hanging wall, minor steeply dipping synthetic faults to the main boundary fault have been observed within Late Jurassic strata which form rotated fault blocks where strata show a general dip towards north (Fig. 3.8). A sedimentary wedge has been observed in Late Jurassic-Early Cretaceous indicating the onset of syn rift deposition during this time (Fig. 3.8A). In the hanging wall all the interpreted reflections are dipping towards the main boundary fault (Fig. 3.8).

On the Loppa High, steeply dipping synthetic and antithetic faults to the main boundary fault have been observed which terminates in the Permian and Carboniferous sequence resulting in the formation of narrow horst and graben geometry (Fig. 3.8). Cretaceous strata onlaps onto the eroded Loppa High in this section as well (Fig. 3.8B).

2D Seismic Line D

This N-S oriented line has been selected from the eastern most part of the study area (Fig. 3.4, Fig. 3.5). The main boundary fault F1 is dipping to the south (Fig. 3.9) and shows a general ENE-WSW trend (Fig. 3.5). Rooted in the basement, this planar fault cuts stratigraphic interval from Carboniferous to Permian. The main boundary fault has a vertical throw of c. 200 ms TWT at Carboniferous level and shows normal geometry (Fig. 3.9). Although, this deep seated fault does not cut strata younger than Permian, however, this provides the mechanism to form a gentle flexure, forming a monocline where all reflections are dipping towards north, in the hanging wall (Fig. 3.9).

In the hanging wall, a set of small synthetic and antithetic faults to the main boundary fault are observed, which form minor horst and graben structures within Jurassic strata (Fig. 3.9). The Hammerfest Basin seems to experience less tectonic activity, evident from the scarcity of faulting (Fig. 3.9). In the footwall, an increase in frequency of faulting is observed. Steeply dipping synthetic and antithetic faults to the main boundary fault with normal geometry, forming narrow horst and graben structures have been observed, in stratigraphic succession from Late Jurassic to Permian (Fig 3.9).

The difference in thickness of strata from Carboniferous to Cretaceous across the Asterias Fault Complex is observed but it is believed to be the result of flexure caused by a deep seated fault giving rise to more accommodation space in the Hammerfest Basin.

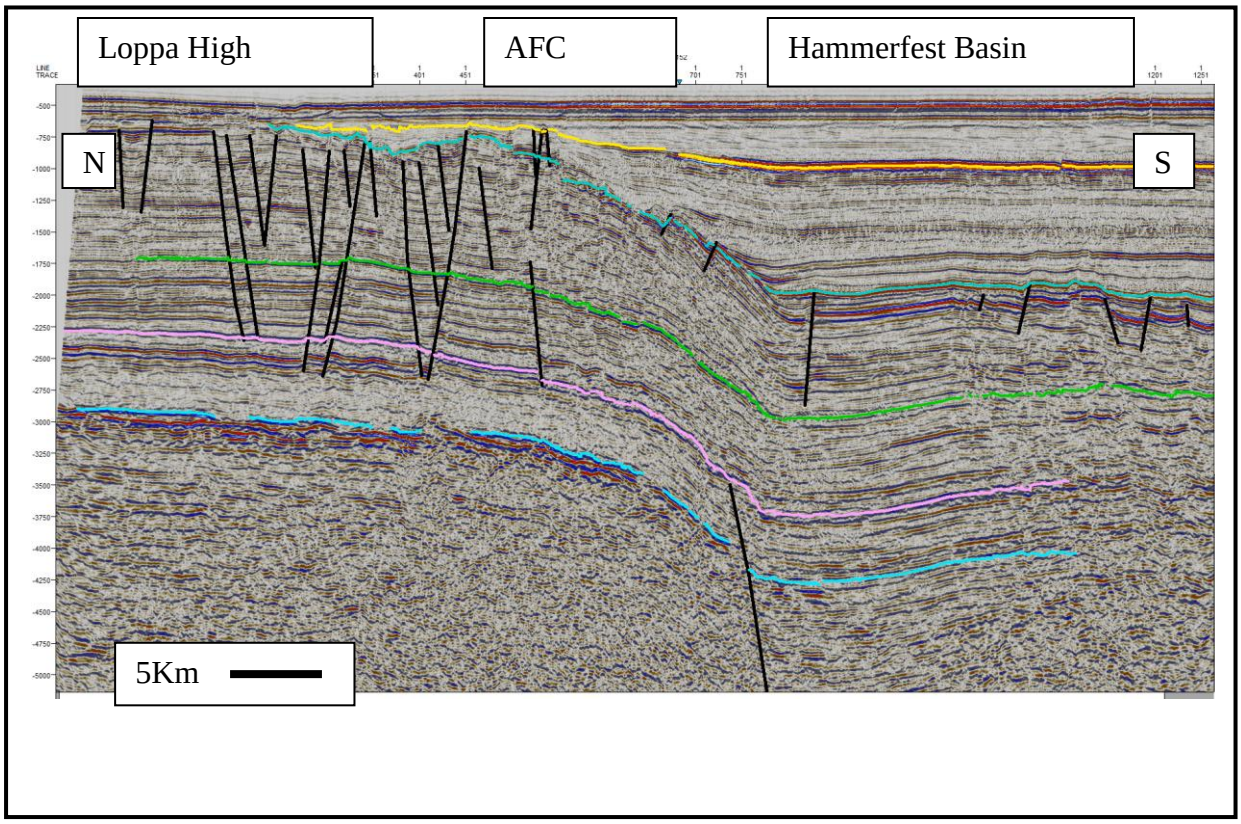

Fig. 3.9: Interpreted 2D seismic Line N-S D (see figure 3.1, 3.4& 3.5 for location) showing deep seated normal fault cutting Intra Permian and forming basis for building up of a gentle flexure. Notice frequency of faulting on Loppa high has increased resulting in the formation of narrow horst and graben geometry (see the colour code for reflections in Table 3.2). See Fig. 3.1 for location.

3.6 3D Seismic Interpretation

A small 3D seismic volume is present in the western part of study area (Fig. 3.1). Two 3D inlines are selected to interpret fault geometry and behavior through space and time.

Inline X

This north-south oriented line is present in western part of the study area (Fig. 3.4 & Fig. 3.5). The main boundary fault (F1) shows staircase geometry in terminology of Gibbs. (1984) and can be divided into three parts (Fig. 3.10):

1) Upper Ramp: steeply dipping to the south

2) Middle Flat: becomes nearly horizontal in Permian strata, a gentle south dip
3) Lower Ramp: steeper than upper ramp, dipping to the south

This fault shows a vertical throw of c. 600 ms TWT with reference to Intra Triassic reflection and cuts stratigraphic succession from Tertiary to the basement (Fig. 3.10), indicating that it is a first or second order structure in terminology of Gabrielsen. (1984).

In the hanging wall (the Hammerfest Basin), a group of two antithetic and one synthetic fault to the main boundary fault (F1) have been observed (Fig. 3.10) displaying normal geometry. Antithetic splay of the main boundary fault cuts stratigraphic sequence from Triassic to the Tertiary and forms half graben evident in Base Cretaceous reflection. While the other group of antithetic and synthetic faults is present within Late Jurassic – Early Cretaceous strata and forms narrow horst and graben structures (Fig. 3.10). Data coverage towards the footwall block of the fault complex is not sufficient to define the geometry of structures there.

In the hanging wall block, the presence of a roll over anticline and associated reverse drag, influencing the stratigraphic sequence from Triassic to the Cretaceous (Fig. 3.10) is observed. This rollover anticline is characterized by the presence of antithetic and synthetic normal faults (Fig. 3.10) which are developed as a response to the continued stretching in the hanging wall during syn-rift phase according to Gibbs. (1984). Thinning of Early Cretaceous strata above the rollover anticline is attributed to the lesser accommodation space available during the time of deposition while this package thickens towards south, away from the rollover anticline (Fig. 3.10).

Inline Y

This north-south oriented line is present in western part of the study area (Fig. 3.4 & Fig. 3.5). Asterias Fault Complex encompasses two normal fault strands (Fig. 3.11). The main boundary fault (F1) shows listric geometry in this profile and shows dip variation with depth i.e., in the Tertiary sequence F1 dips steeply to the south while in the Permian sequence this fault flattens with a gentle south dip (Fig. 3.11). The other master fault (F2) is planar in nature and dips to the south (Fig. 3.11).

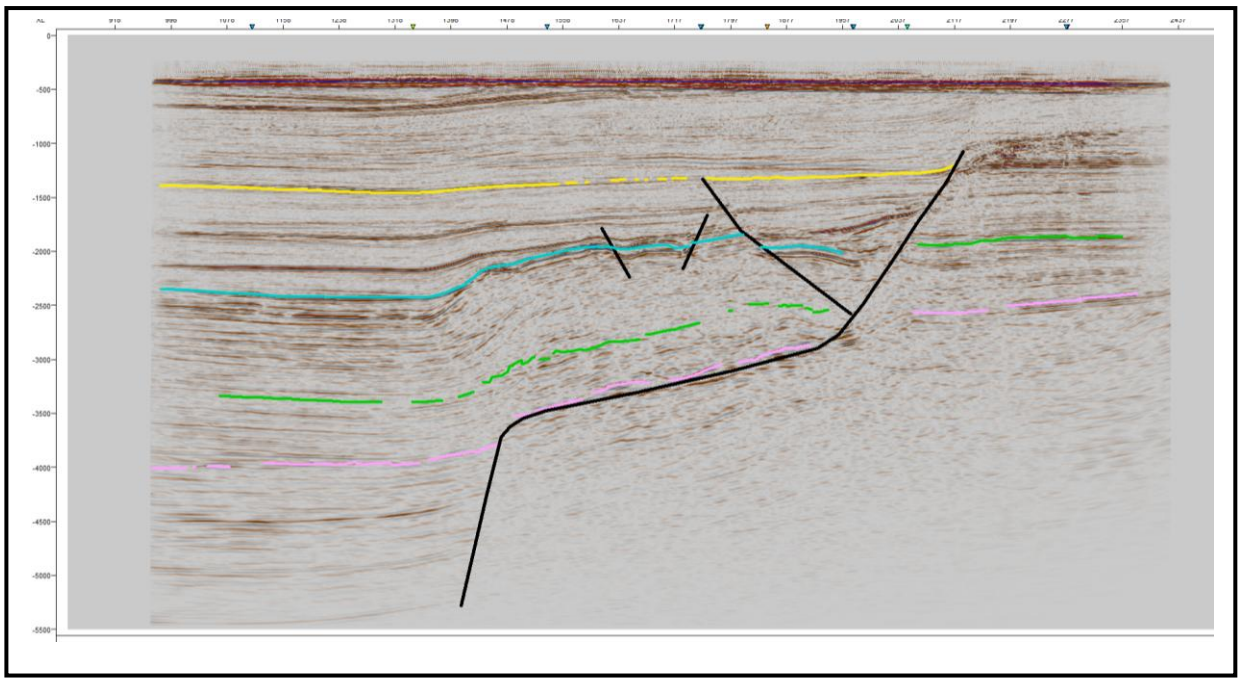

Fig. 3.10: Interpreted 3D seismic Inline X (see figure 3.4& 3.5 for location) showing listric fault normal flatten in Permian strata making it a detachment horizon (see the colour code for reflections in Table 3.2).

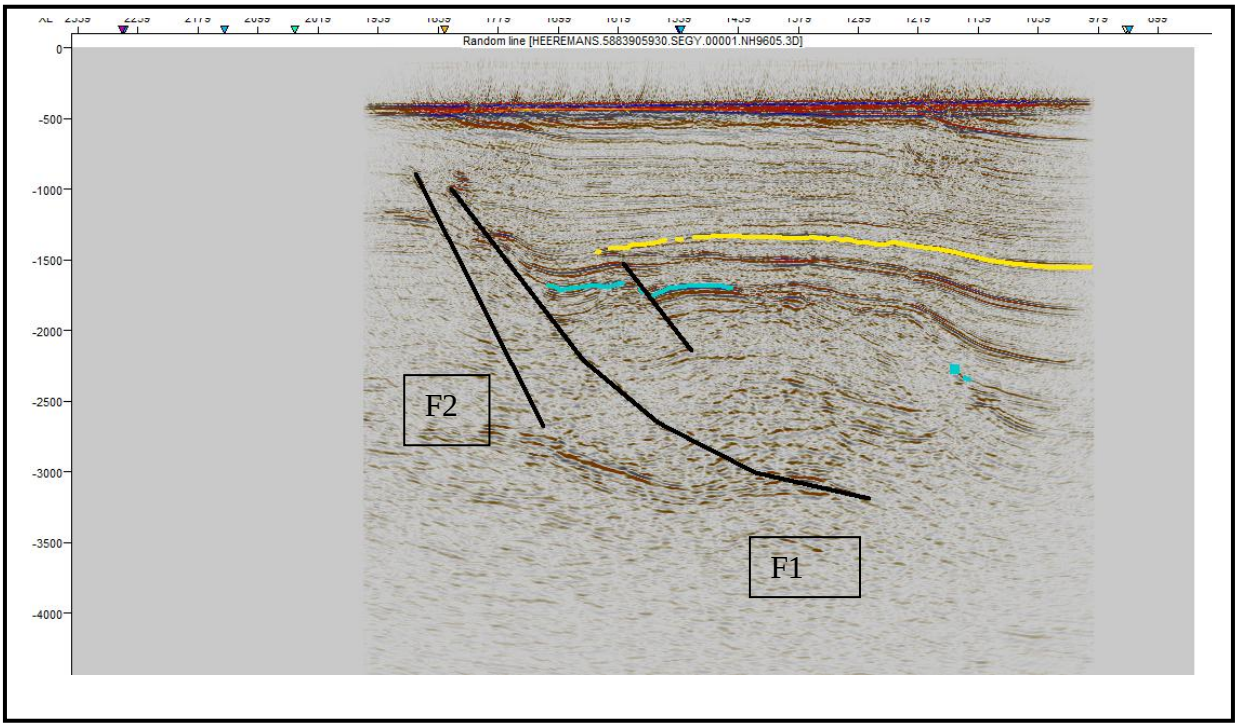

Fig. 3.11: Interpreted 3D seismic Inline Y (see figure 3.4& 3.5 for location) showing listric fault normal flatten in Permian strata making it a detachment horizon (see the colour code for reflections in Table 3.2).

The main boundary fault cuts stratigraphic succession from Early Tertiary to the Permian (Fig. 3.11), while it seems to have flatten in Permian strata making it a detachment horizon. In the hanging wall (the Hammerfest Basin) a synthetic fault to the main boundary fault (F1) has been observed (Fig. 3.11). The hanging wall in this profile however, lacks the presence of reverse drag, rather normal drag is found to be associated with the rollover anticline (Fig. 3.11). Although, rollover anticline is not fully developed in this section however, there is sufficient evidence, such as presence of bi-directional dip of strata within the Triassic sequence, to support the idea of rollover anticline in the hanging wall block (Fig. 3.11). Thinning of Early Cretaceous strata above the rollover anticline is attributed to the lesser accommodation space available above rollover, at the time of deposition while this package thickens towards south (Fig. 3.11).

3.7 Description of Time Structure & Fault Maps

Time structure maps have been generated at five levels including Intra Carboniferous, Intra Permian, Intra Triassic, Base Cretaceous and Base Tertiary. Similarly, fault maps have also been generated at four levels including Intra Carboniferous, Intra Permian, Intra Triassic and Base Cretaceous.

Intra Carboniferous

Time structure map and fault map at Intra Carboniferous level shows that ENE-WSW trending main boundary fault dip steeply to the south east (Fig. 3.12a,b). Vertical separation down to the south of the western compartment of the Asterias Fault Complex is greater as compared to its eastern compartment (Fig. 3.12a). General structural trend on the western side of footwall is NNE-SSW which marks the paleo-high, while towards the eastern side of footwall ENE-WSW trend dominates (Fig. 3.12b). In the hanging wall ENE-WSW trends have been observed towards western side defining the half graben (Fig. 3.12a, Fig. 3.6). On the footwall, horizon gently dips southward towards the Asterias Fault Complex while in hanging wall; the horizon dips north. High time values in the southwestern part of the study area marks the deepest part and it is inferred that this area has experienced maximum subsidence with the development of Asterias Fault Complex.

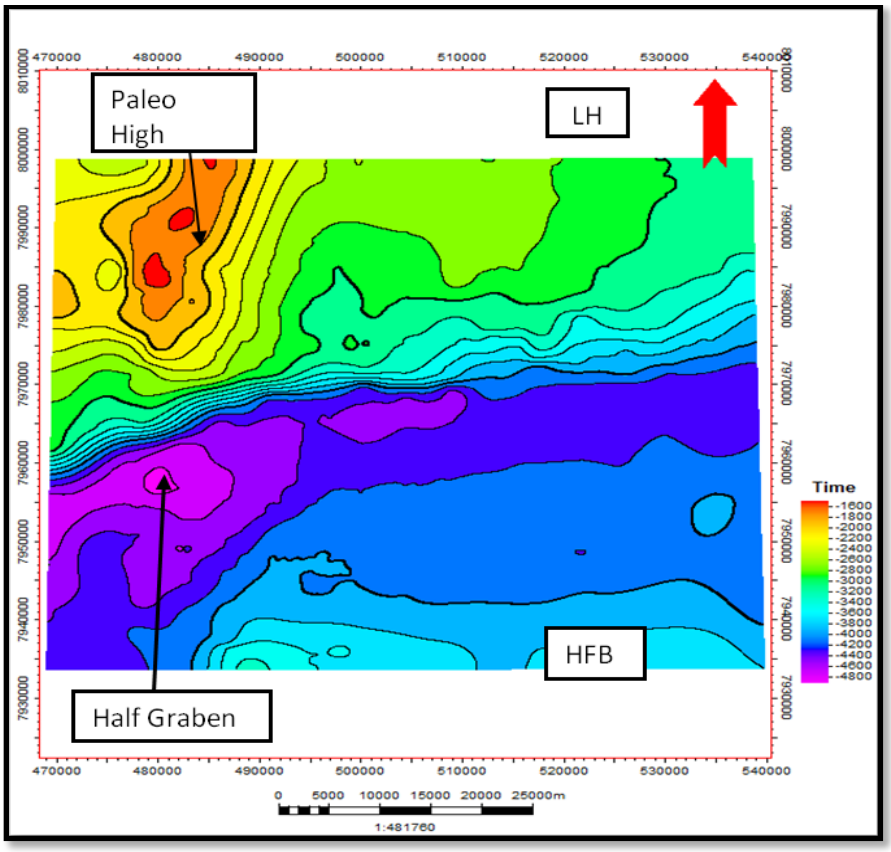

Fig. 3.12a Time -Structure map at Intra Carboniferous level HFB: Hammerfest Basin LH: Loppa High. Northwestern part showing paleo-high on footwall of Asterias Fault Complex.

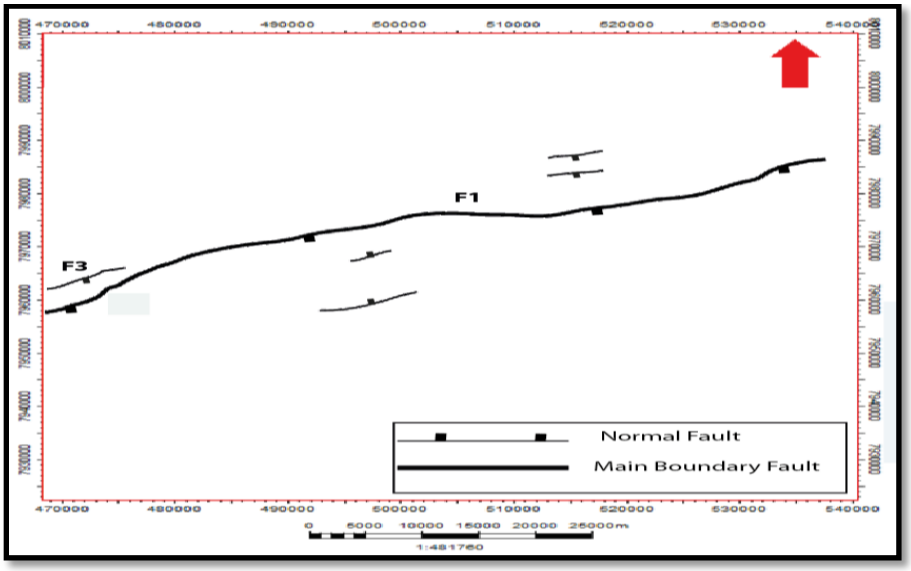

Fig 3.12b: Fault map at carboniferous level F1is the main boundary fault.

Intra Permian

Time structure map and fault plane map at Intra Permian, reveals that ENE –WSW trending main boundary fault F1 terminates in the east while it dips to the south-east (Fig. 3.13a,b). Time values across the Asterias Fault Complex show that vertical separation down to the south in the western compartment of the Asterias Fault Complex is greater as compared to its eastern compartment (Fig. 3.13A). The NE-SW trend in the eastern side of the footwall is defining narrow grabens (Fig. 3.13a & Fig. 3.9) where as NS trend in western side of foot wall defines the paleo-high (Fig. 3.13a & Fig. 3.6). In the hanging wall, ENE-WSW structural trends have been observed towards the western side defining the half graben (Fig. 3.13a). Northern flank of hanging wall and southern flank of footwall is dipping towards main boundary fault (Fig 3.7). In the hanging wall, western side shows greater time values as compared to the eastern side, pointing that western side has experienced more subsidence at Intra Permian level. Intra Permian is eroded from the northwestern part of the study area on the paleo-high, however, contouring algorithm of Petrel (software) assumes certain value instead of zero which is shown as red (Fig. 3.13a).

Intra Triassic

Time structure map and fault plane map shows that structural elements at Intra Triassic level are similar to the structural elements observed at Intra Permian level. ENE-WSW main boundary fault is dipping towards southeast (Fig. 3.14a & Fig. 3.14b). The footwall towards east is characterized by a narrow graben trending ENE-WSW (Fig. 3.9 & Fig. 3.14b). Significant contrast in time values on western and eastern sides of Hanging wall and footwall explains the differential subsidence experienced by the hanging wall which is more pronounced towards west (Fig. 3.14a).

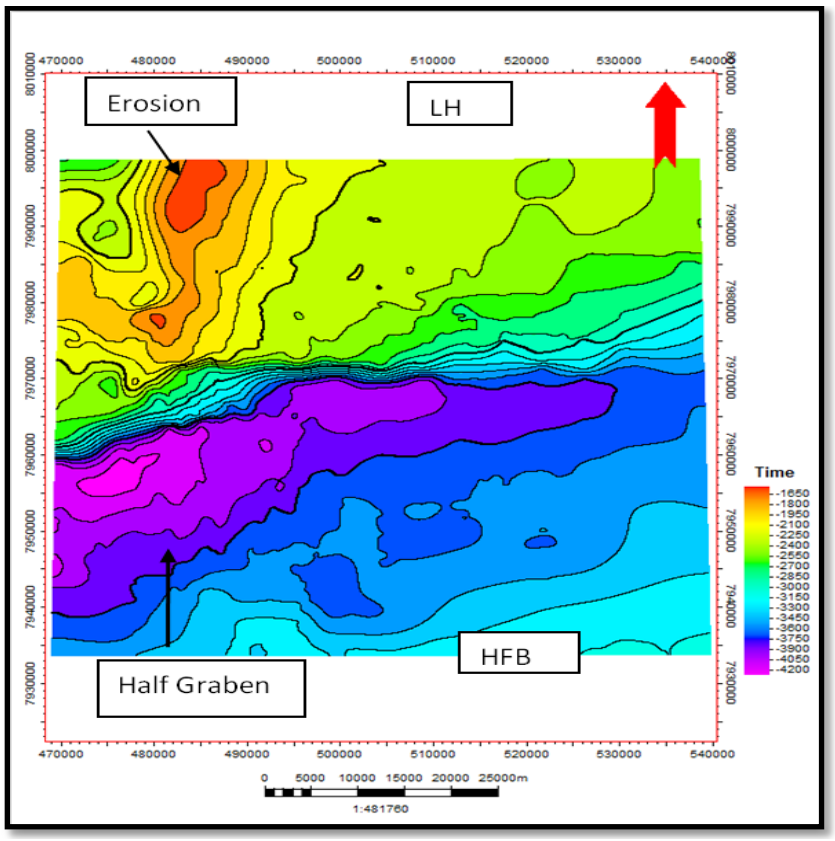

Fig. 3.13a: Time- Structure map at Intra Permian level HFB: Hammerfest Basin LH: Loppa High. Notice contrasting trends in strike of the Intra Permian horizon on footwall and hanging wall of the fault complex.

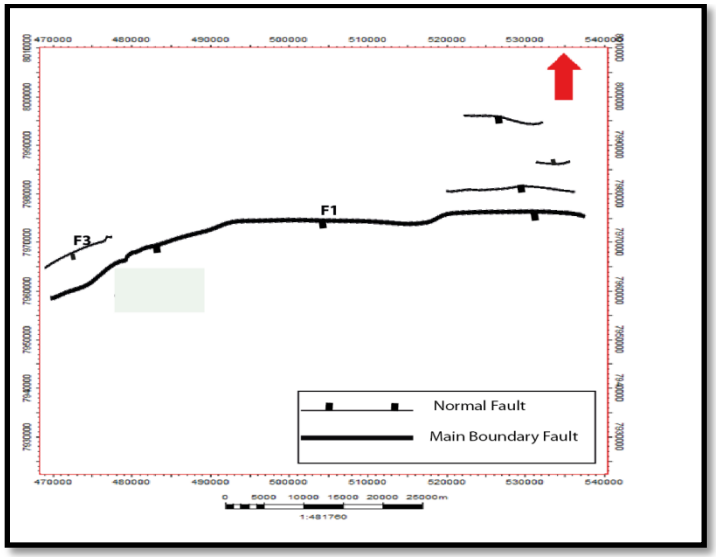

Figure 3.13b: Fault map at Permian level F1is main boundary fault

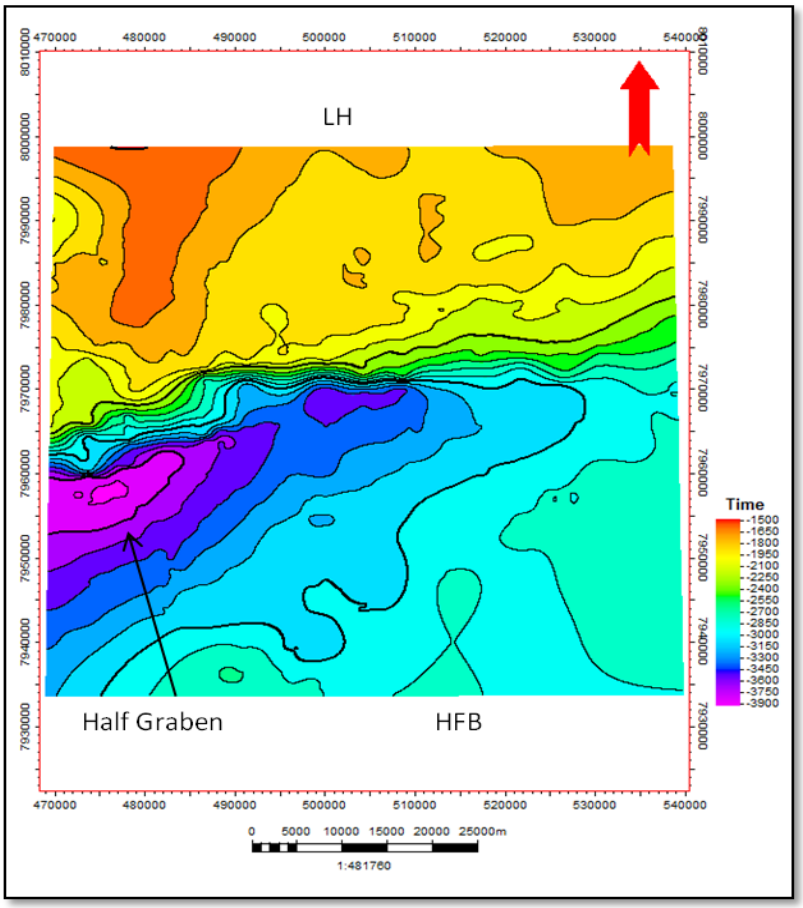

Fig. 3.14a: Time- Structure map at Intra Triassic level HFB:Hammerfest Basin LH:Loppa High, southwestern part of study area is the deepest part showing greater time values in hanging wall of the fault complex. Notice the difference in contour trends on footwall and hanging wall across the fault.

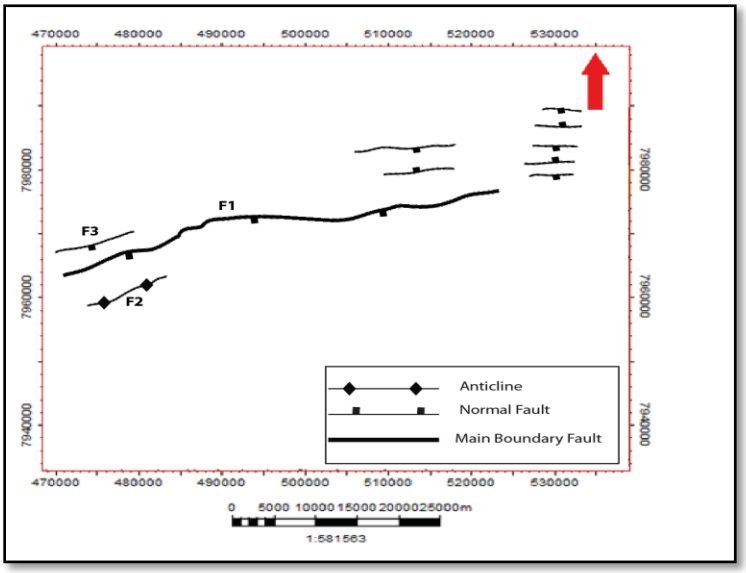

Figure 3.14b: Fault map at Triassic level F1 is the main Boundary Fault

Base Cretaceous

Time structure map is divided into three segments depending upon the structural trend and complexity observed at the base Cretaceous level. Western segment has greatest influence of antiformal feature that gradually becomes less pronounced towards central segment and eventually diminishes towards eastern segment (Fig. 3.15b). Asterias Fault Complex shows WSW–ENE to EW trend on fault plane map at Base Cretaceous level (Fig 3.15a,b). An anticlinal structure can be observed on the western side showing NE-SW trend and which has been absent on the previous time structure maps (Fig. 3.15a). Time structure maps at Intra Carboniferous & Intra Permian level show subsidence in the close proximity of Asterias Fault Complex on western side of the study area, whereas time structure map at Base Cretaceous level at the same location reveals the presence of an anticlinal feature that is interpreted as a roll-over anticline which controls thickness of Cretaceous strata. This anticlinal feature has also been observed in cross sections of this part as well (Fig. 3.6 & Fig. 3.7). The northwestern flank of Hammerfest Basin dips towards north, showing subsidence with the development of Asterias Fault Complex.

Base Tertiary

Base Tertiary is the shallowest reflection that has been interpreted in the study area (Fig. 3.7 & 3.8). E-W trending main boundary fault F1 terminates towards east (Fig. 3.8 & Fig. 3.16). Time structure mapping reveals that eastern part experienced rather smooth deposition with no influence of faulting. Towards western part of hanging wall no anticlinal feature is observed at this level suggesting that deposition of Tertiary sequence was not controlled by the underlying rollover anticline. Northwestern flank of the Hammerfest Basin shows large time values contrast as compared to the eastern side making it an area of greater subsidence at this time.

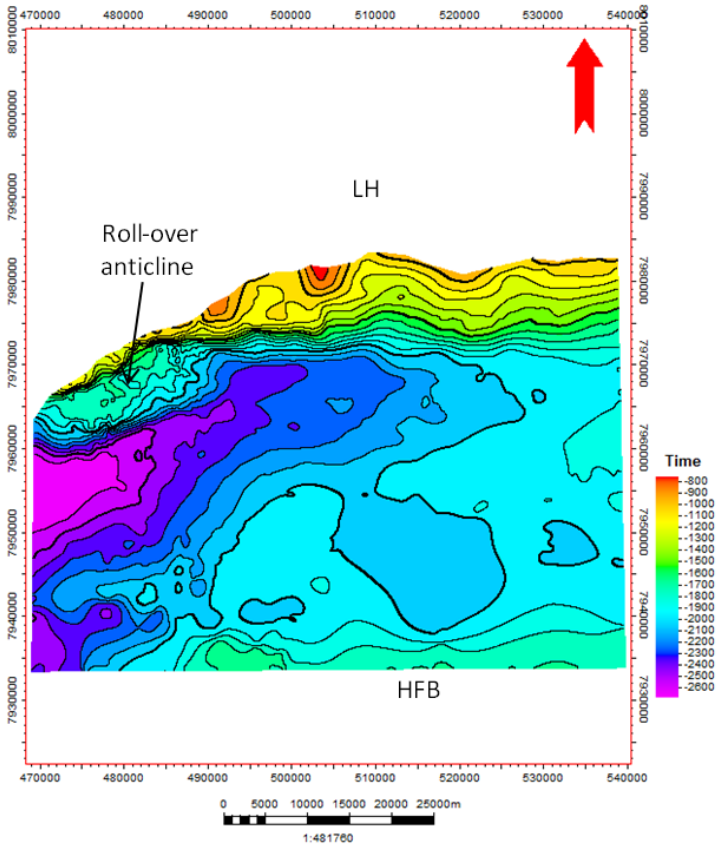

Fig 3.15a: Time -Structure map at Base Cretaceous level HFB: Hammerfest Basin LH: Loppa High. Notice missing Cretaceous strata on western Loppa High due to uplift

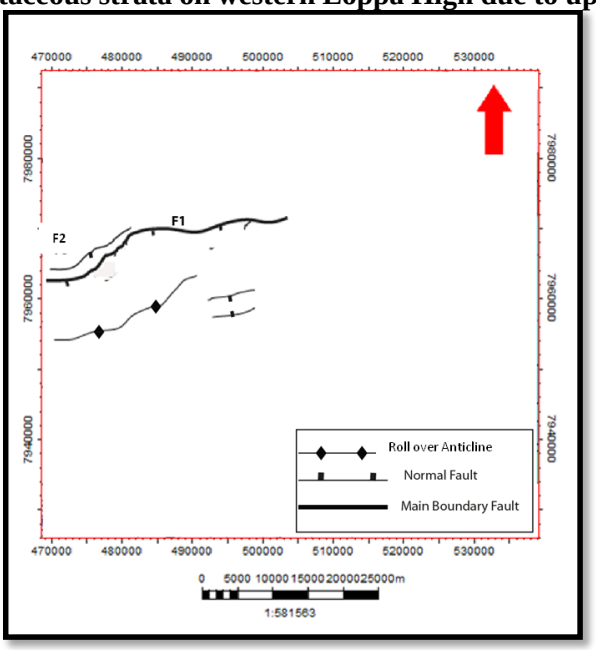

Figure 3.15b: Fault map at Base Cretaceous Level. F1 is the main Boundary Fault

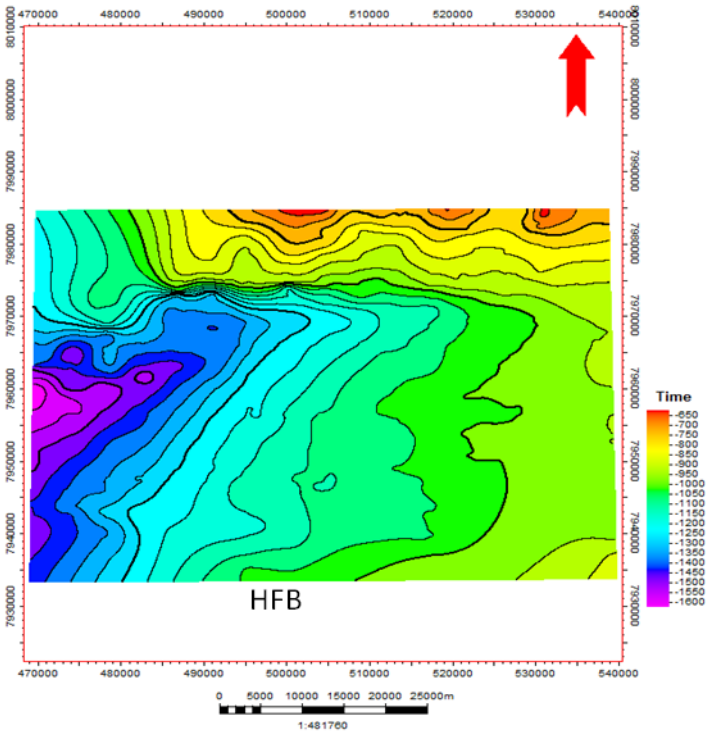

Fig 3.16: Time-Structure map at Base Tertiary level HFB: Hammerfest Basin LH: Loppa High. Notice missing Early Tertiary strata on western Loppa High due to uplift.

4 Discussion

On the basis of structural trend and complexity, the Asterias Fault Complex is divided into three compartments, namely the western, the central and the eastern, which exhibit varying degree of deformation (faulting and fault related structuring and vertical displacement along fault) that decreases in intensity from west to east.

The western compartment of the Asterias Fault Complex presents a challenge to interpret the governing stress system which resulted in the formation of an associated local uplift / bulge (Fig 3.10 & Fig 4.1). This antiformal feature can be explained as the product of three virtually different structural configurations, folding related to compression, half flower structure or rollover anticline. Viability of each configuration is evaluated in this chapter and conclusion is drawn by selecting the best fit stress model, responsible for shaping the western segment of the Asterias Fault Complex. Therefore, the plausible structural configurations presented in the hypothesis are elaborated in this section to evolve the understanding about true nature of the stress system resulting in formation of present fault geometry of western compartment. Discussion then follows the structural style of the Asterias Fault Complex as it is divided into three segments namely (i) The Western segment (ii) The Central segment and (iii) The Eastern segment. Finally, geological evolution of the fault complex is discussed through different time periods.

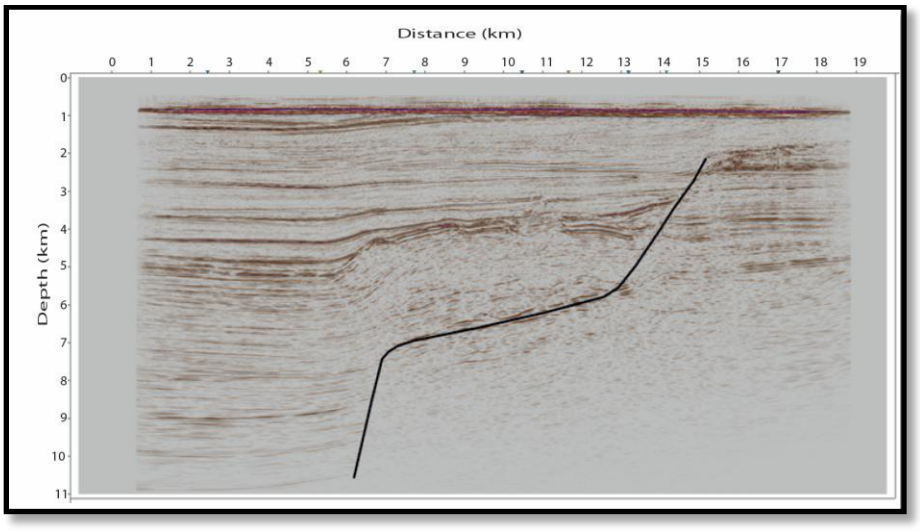

Figure 4.1: Depth converted seismic inline X showing antiformal feature in the hanging wall block of the fault, different structural configuration are assessed to explain this feature. Vertical and horizontal distance are same

4.1 Model 1 – Tectonic inversion related to compressional stress system

In order to evaluate the fault geometry and related structural style of the western compartment of the Asterias Fault Complex, tectonic inversion is taken as first candidate for governing the fault geometry in this section. Positive inversion deals with the concept of slip reversal along pre-existing normal faults under the influence of compressional stresses (Bally 1984) (Fig 4.1). Areas bearing contractional signatures can be found locally within regional extensional or strike slip regimes. Such areas are characterized by presence of folds and reverse/thrust faults which make up basic elements of this stress regime (Gabrielsen 2010).

Western compartment of the Asterias Fault Complex does not bear sign of compressional system as it clearly lacks low angle thrust faults and fault propagation folds (compressional sense) during Late Jurassic-Early Cretaceous period. On the contrary, however, the main boundary fault of Asterias Fault Complex shows normal dip slip at Jurassic-Cretaceous transition and abundance of synthetic and antithetic faults to the main boundary fault also manifest normal geometry (Fig 3.7 & Fig 3.10). Therefore, the possibility of compressional stresses to generate the antiformal feature in the western compartment of the Asterias Fault Complex is ruled out.

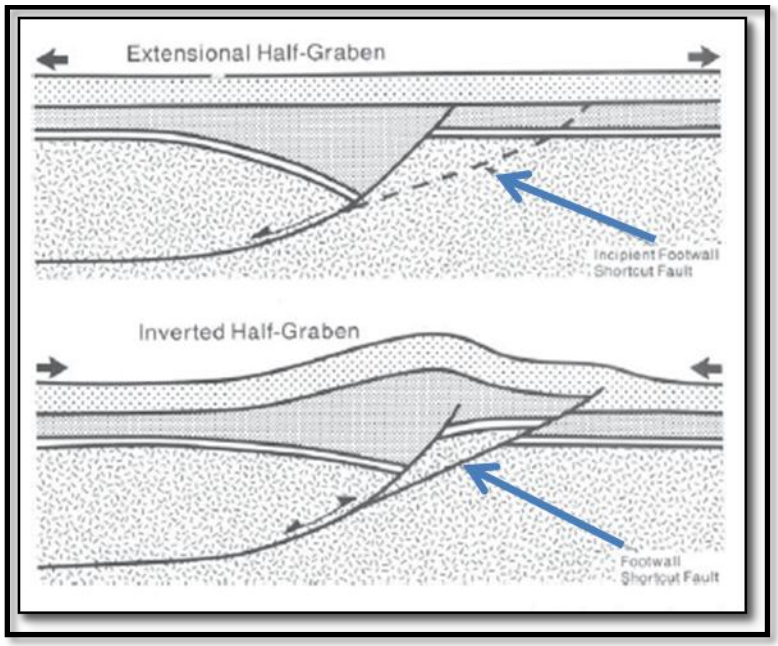

Fig 4.2: Sequential development of positive inversion showing slip reversal on pre-existing normal fault resulting in formation of uplift / bulge (modified from Cooper et al., 1989). Footwall shortcut faults are absent in western segment of Asterias Fault Complex.

4.2 Model 2 – Strike-Slip System

Transpressional stress system is taken as second possible candidate for generating the complex fault geometry in western segment of the Asterias Fault Complex. Previous literature supports the idea of half flower structure and local doming in the western compartment of the study area as described by Berglund et al. (1986). Rønnevik et al. (1984) related this inversion to Late Jurassic wrenching in the western and northern Barents Sea. Dextral strike-slip movement is suggested to have caused the local compression and formation of half flower structure at the end of Jurassic times by Berglund et al. (1986) whereas, Ziegler et al. (1986) proposed a dextral gravity induced movement for the formation of this structure. Gabrielsen et al. (1993) dated the inversion to Hauterivian and suggests that definite proof of strike slip movement is inadequate and recommends looking for other possible mechanisms for the formation of such a structure.

Profile characteristics of the positive flower structure is a linear antiform that is bounded longitudinally at flanks by upward and outward diverging strands of wrench fault that have mostly reverse separation (Harding and Lowell, 1979; Harding 1985) (Fig 4.2). However, the present study does not warrant the interpretation of this uplift / bulge as a half flower structure (Fig 3.6 & Fig 3.11). Particularly, inclusion of 3D seismic data set during interpretation revealed clear signatures for the absence of any strike slip related feature in the western segment of the fault complex (Fig 3.10). Lack of evidence of strike slip movement in the regional tectonic context during Early Cretaceous together with reflection seismic data not supporting the scheme of strike slip system, suggests looking for other viable mechanism for this uplift / bulge in the western segment of the Asterias Fault Complex.

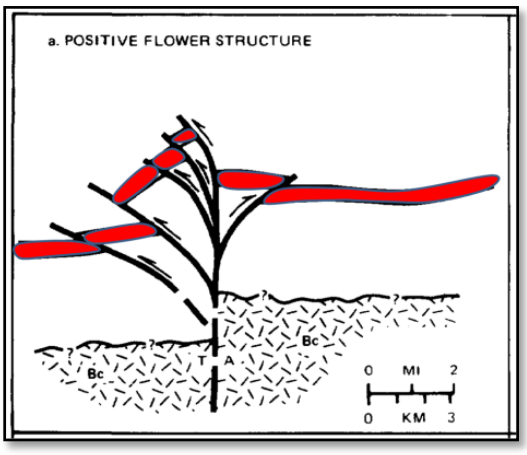

Fig 4.3: Positive flower structure modified from Harding (1985).

4.3 Model 3 – Extensional System "Roll-over Anticline associated with Listric Fault"

Extensional stress system is the final candidate to have evolved the geometry associated with the western segment of Asterias Fault Complex. Besides the formation of planar normal faults, extensional stresses can lead to the formation of listric curved faults as well. In extensional regimes, roll-over anticline forms as a result of listric faulting and reverse drag (Hamblin, 1965) (Fig 4.3). Antithetic or counter faults to the master fault are developed in the hanging wall, and strata involved within the roll-over becomes thin (Gibbs, 1984). In some cases however, the extreme curvature of antithetic fault can lead to the development of local compressional stress and generation of a drag and reverse fault (Gibbs, 1984). Roll- over geometry can be used to construct the change in the curvature of the plane of listric fault (Gibbs,1983). However in present study dips at various points on the plane of listric fault are computed. Similarly, presence of rollover anticline is evaluated by projecting values of vertical and horizontal separation on the reference datum which will support or negate the idea of rollover anticline forming the antiformal feature associated with the western segment of the Asterias Fault Complex.

4.3.1 Fault plane profile of the master fault

3D seismic inline X was depth-converted assuming average velocity of 4km/sec (Fig 4.1). Vertical scale is given in TWT which is converted to depth using the equation S= vt/2. After the depth conversion of vertical scale, 500ms TWT on section corresponds to 1 km (Fig4.5). Horizontal scale is adjusted so as to obtain a similar vertical and horizontal scale. Distance between two cross lines is 12.50m, therefore, difference of 80 cross-lines correspond to 1km.

Ten points were selected on the fault plane and the vertical separation (t) and heave (h) were calculated (Fig4.5). Fault dips were then computed for the depth converted section with (1:1) scale (Table 4.1). Dip values show a systematic decrease in amount from c. 50^0 in the upper part to 12^0 in the central part and then increases to c.60^0 in the deepest part of the fault seen in the seismic section (Table 4.1). This change in dip of fault plane dips, from higher to lower and higher again illustrates the real ramp-flat-ramp fault geometry similar to that discussed in Gibbs (1984). Such fault plane geometry can explain the development of uplift / bulge present in the

western part of Asterias Fault Complex by introducing the concept of roll-over anticline (Fig 3.10, Fig. 4.1) associated with the listric fault.

During interpretation, Intra Permian is picked within the Røye Formation which is characterized by interbedded silicified marls, silty carbonate mudstone and calcareous mudstone (Larsen et al. 2002). This calcareous mudstone may act as a detachment horizon for the development of "flat" in ramp-flat geometry (Fig 3.10).

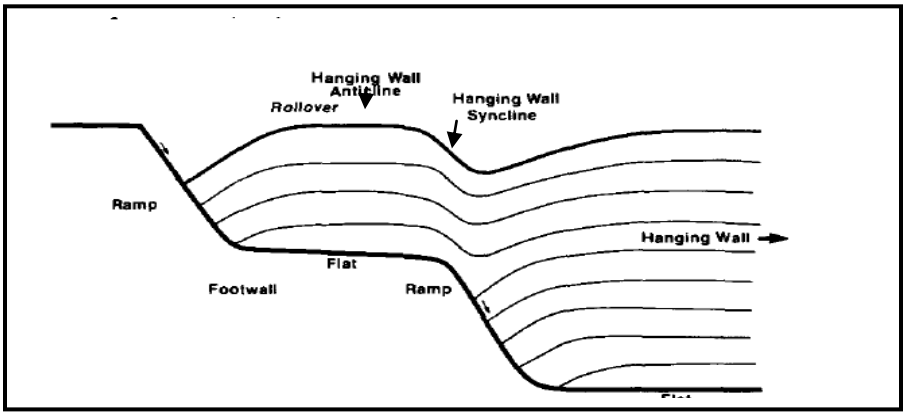

Figure 4.4: Rollover anticline and Ramp flat geometry (modified from Gibbs 1984)

No of Obs.	Throw (km)	Heave(km)	Dip (degree)
1	0.5	0.4	51
2	0.5	0.5	45
3	0.5	0.6	39
4	0.5	0.4	51
5	0.3	1	16
6	0.3	1.4	12
7	0.3	1.4	12
8	0.3	0.4	36
9	1	0.5	63
10	1	0.5	63

Table 4.1: Throw, Heave and Dip values calculated at various points on a listric fault, dip is calculated using $\tan\theta = t/h$ (Gibbs 1983)

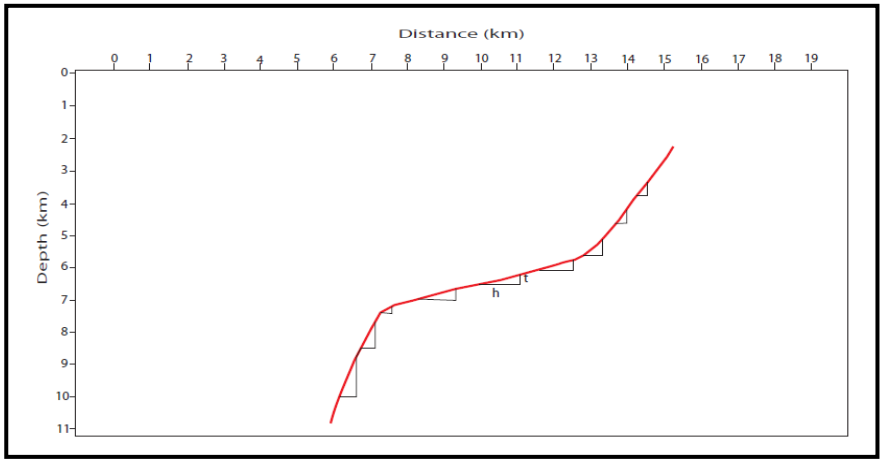

Fig 4.5: Depth converted 3D seismic inline X showing listric fault throw(t) & heave(h) calculated at random points on fault plane.

4.3.2 Shape of rollover anticline

In order to control whether the observed hangingwall roll-over geometry can be explained by the existing ramp-flat-ramp fault geometry alone a geometric analysis of, a depth-converted version of 3D seismic inline X was undertaken (Fig 4.6), using the principles of Gibbs (1984). Fault throws (t) and heaves (h) were computed at uniform intervals and projected onto a reference horizontal plane, which corresponds to the base of the post rift sequence (Fig 4.6). Vertical displacement for every point on the reference datum is same as its corresponding throw (t) and the horizontal distance between two points is equal to the heave (h) computed on the fault plane (Fig 4.6) i.e., greater throw (t) at fault plane equals the greater vertical displacement from reference datum and vice versa. After projecting all points from reference datum vertically downward, they were joined and the resultant geometry assumed the shape of a rollover anticline (Fig 4.6). Resultant rollover anticline bears close resemblance with the rollover anticline explained by Gibbs (1984) (Fig 4.4). This feature is then compared with rollover anticline seen on the depth converted seismic inline X and clear similarity is observed (Fig 4.6b). This rollover anticline gives practical solution to the complexity associated with the western compartment of Asterias Fault Complex in the form of a local uplift / bulge, explaining that uplifted part / bulge seen on reflection seismic of western part of the fault complex is not result of inversion tectonics related to compressional or transpressional stress system rather it is listric normal fault within extensional stress regime that governs the structural grain of the western compartment of the Asterias Fault Complex (Fig 3.10).

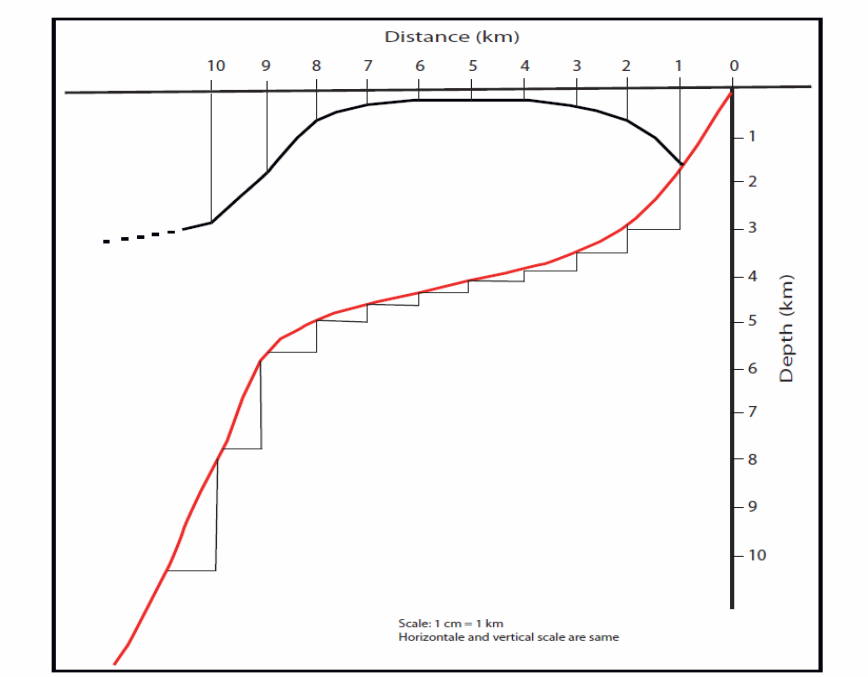

Fig 4.6: Fault plane from depth converted 3D seismic inline X showing rollover anticline constructed by projection of throw(t) & heave(h) information on reference datum and plotting throw (t) values vertically downward.

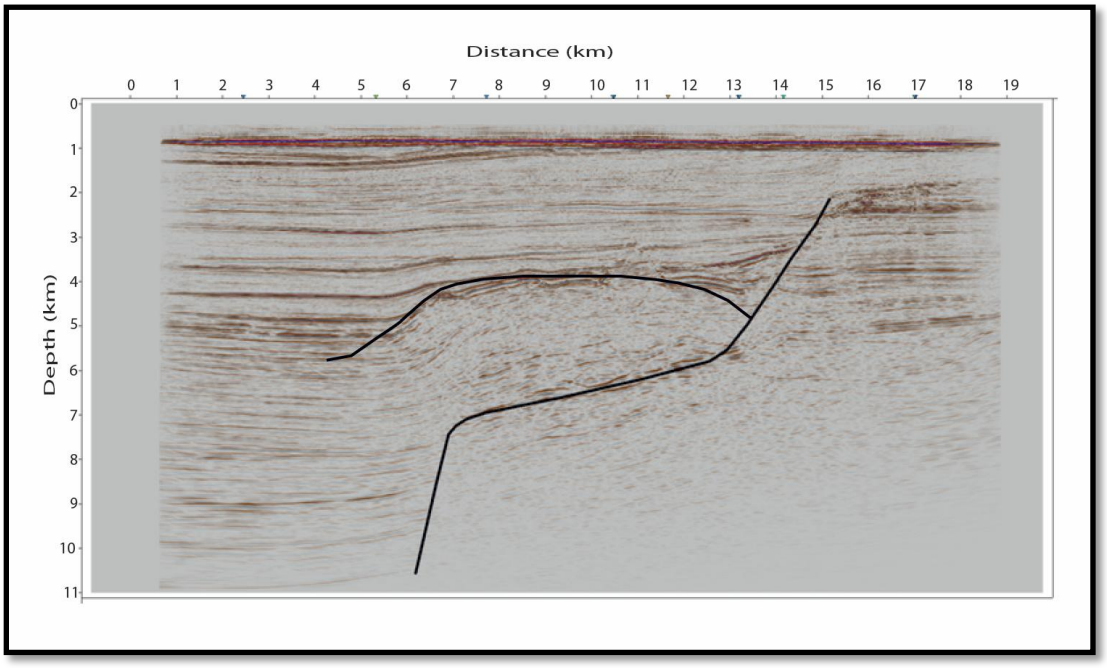

Fig 4.6b: Comparsion betweem the constructed roll-over anticline by projecting throw and heave information with the roll-over anticline seen on the depth converted 3D seismic inline X.

4.4 Structural Style of Asterias Fault Complex

The Asterias Fault Complex separates the Loppa High in the north from Hammerfest Basin towards the south (Gabrielsen et al., 1990). During present study, the Asterias Fault Complex is subdivided into a western, a central and an eastern segment on the basis of geometry and structural trend identified at Base Cretaceous level (Fig 3.4 & Fig 3.5). The western segment strikes ENE-WSW (Fig 3.5) and consists of ramp- flat geometry associated with listric normal fault (Fig 3.10). This segment defines the junction of Asterias Fault Complex with the Ringvassøy-Loppa Fault Complex and accommodates the deepest part of the study area, identified on time-structure and thickness trend map (Fig 3.15a & Fig 4.9). The central segment strikes E-W (Fig 3.5) and ramp -flat geometry is not fully developed in this segment instead downward concave fault is observed, however, still the effect of development of roll-over anticline is observed (Fig 3.7). Towards the eastern segment listric geometry of the master fault leads way to the planar normal fault which strikes ENE-WSW (Fig 3.5). Eastern segment does not bear signs of development of a roll-over geometry in the hanging wall primarily due to planar nature of the fault and also that planar fault is deep seated in this segment cutting strata from Carboniferous to Permian (Fig 3.9). Intensity of faulting decreases from western to eastern segment (3.15b) and basin depth becomes shallower in the similar fashion (Fig 3.15).

4.4.1 The western segment of the Asterias Fault Complex

The western-most segment of the Asterias Fault Complex consists of two large master faults trending ENE- WSW and dipping predominantly to the south-east (Fig 3.15a & Fig 3.15b). The fault F3 is a planar normal fault dipping south-east while it terminates in the Carboniferous strata (Fig 3.6). The fault F1 shows ramp-flat geometry, dips to south-east and is probably rooted in the basement (Fig 3.6 & Fig 3.10). This observation is quite consistent with the observations of Gabrielsen et al. (1984).

The profile characteristics of the fault F1marks a ramp- flat geometry in the terminology of Gibbs (1984) (Fig3.10). Upper ramp of the fault F1 is associated with the roll-over anticline affecting the strata from Late Permian to Early Cretaceous (Fig 3.10). Calcareous mudstone of Røye Formation may have provided the decollement zone and favored formation of “flat”

geometry within Permian strata (Fig 3.10). Deeper down, the fault geometry transforms again into the ramp and dip becomes higher (Fig 3.10).

Roll-over anticline in the hanging wall of fault F1 formed as a result of Late Jurassic – Early Cretaceous extension on listric normal fault F1. Time structure map at Base Cretaceous level, towards northwestern part is characterized by the presence of a roll-over anticline as well (Fig 3.10). Development of growth strata in Early Cretaceous has been recognized (Fig 3.6 & Fig 3.10) on the basis of which roll-over anticline associated with the fault F1 is assigned the age of Early Cretaceous. This roll-over anticline is responsible for thinning of lower Cretaceous strata over the anticline due to lesser accommodation space while towards south the thicknesses of this package increase (Fig 3.6).

The normal synthetic and antithetic faults in the hanging wall of Fault F1 are also observed (Fig 3.6 & Fig 3.10) cutting strata from Late-Triassic to Late Jurassic, these faults are formed as a result of continued extension along the main boundary fault F1 which gives way to the formation of accommodation structures in the hanging wall.

4.4.2 The Central Segment of Asterias Fault Complex

The ramp flat geometry gives way to downward concave fault in this segment (Fig 3.7). This segment is characterized by the E-W trending normal fault (Fig 3.15b). Roll-over anticline related with downward concave fault F1, is less pronounced in this segment while its effect diminishes further east. Presence of growth strata has been recognized near the Base Cretaceous reflection indicating the onset of rifting in Late Jurassic – Early Cretaceous period (Fig 3.8). In the Hammerfest basin rotated fault blocks have been observed at Mid Jurassic level (Fig 3.8), where faults are synthetic to the main boundary fault and the strata shows a general to the north dip. The Loppa High is characterized by narrow horst and graben system and noteworthy feature of this segment is reduction in fault frequency in the Hammerfest Basin as compared to the Loppa High (Fig 3.8).

4.4.3 Eastern Segment of Asterias Fault Complex

Listric fault and associated roll-over anticline is totally absent in this segment (Fig 3.9). A deep seated normal fault that does not cut younger strata than Permian is identified which provides the mechanism to form a gentle flexure towards hanging wall. This flexure helps in shaping overall geometry of the Hammerfest Basin to appear as a monocline, (Fig 3.9) where all reflections show a general north dip. Difference in thickness of strata from Carboniferous to Cretaceous across the Asterias Fault Complex is believed to be controlled by a fault at depth giving rise to more accommodation space in the Hammerfest Basin (Fig 3,9 & Fig 3.15b). In this segment, Loppa high is characterized by narrow horst and graben striking EW which terminates at Permian level (Fig 3.9, 3.13b & 3.14b). However, like the central segment, this segment too, witnesses low fault activity in the Hammerfest basin (Fig 3.9).

4.5 Geological Evolution of the Asterias Fault Complex

The evolution of Asterias Fault Complex is studied through the observation of tectonics (subsidence and uplift), erosion and deposition on the seismic reflection data.

4.5.1 Mid Carboniferous to Early Permian

Late Devonian to Mid-Carboniferous was a period of extensive rifting in the Barents Sea (Gabrielsen et al., 1990; Gudlaugsson et al., 1998). Whereas, Early Permian was characterized by post-rift phase and regional sag basins developed on the Barrents Shelf (Gudlaugsson et al., 1998; Faleide et al., 2010). E-W extensional regime dominated the Hammerfest Basin with reactivation of underlying basement faults such as a major fault zone beneath the present day Ringvassøy Loppa Fault Complex (Berglund et al., 1986).

Time-thickness map between Intra Carboniferous and Intra Permian reflections show homogeneity in terms of thickness on the eastern side of the study area but decrease in the thickness is observed on the western side of the Loppa High (Fig 4.7). On the Loppa High, an important observation is presence of Early Permian strata south of the paleo-high which has approximately similar thickness as that of across the main boundary fault in the hanging wall (the Hammerfest Basin), which implies that during Early Permian paleo-high did not exist and

uplift took place later resulting in erosion of Early Permian strata on top of the paleo-high (Fig 3.6 & Fig.4.7). Similarly, no growth strata has been observed in the interval between Intra Carboniferous- Intra Permian on 2D seismic reflection data which in turn points to lack of any rift episode.

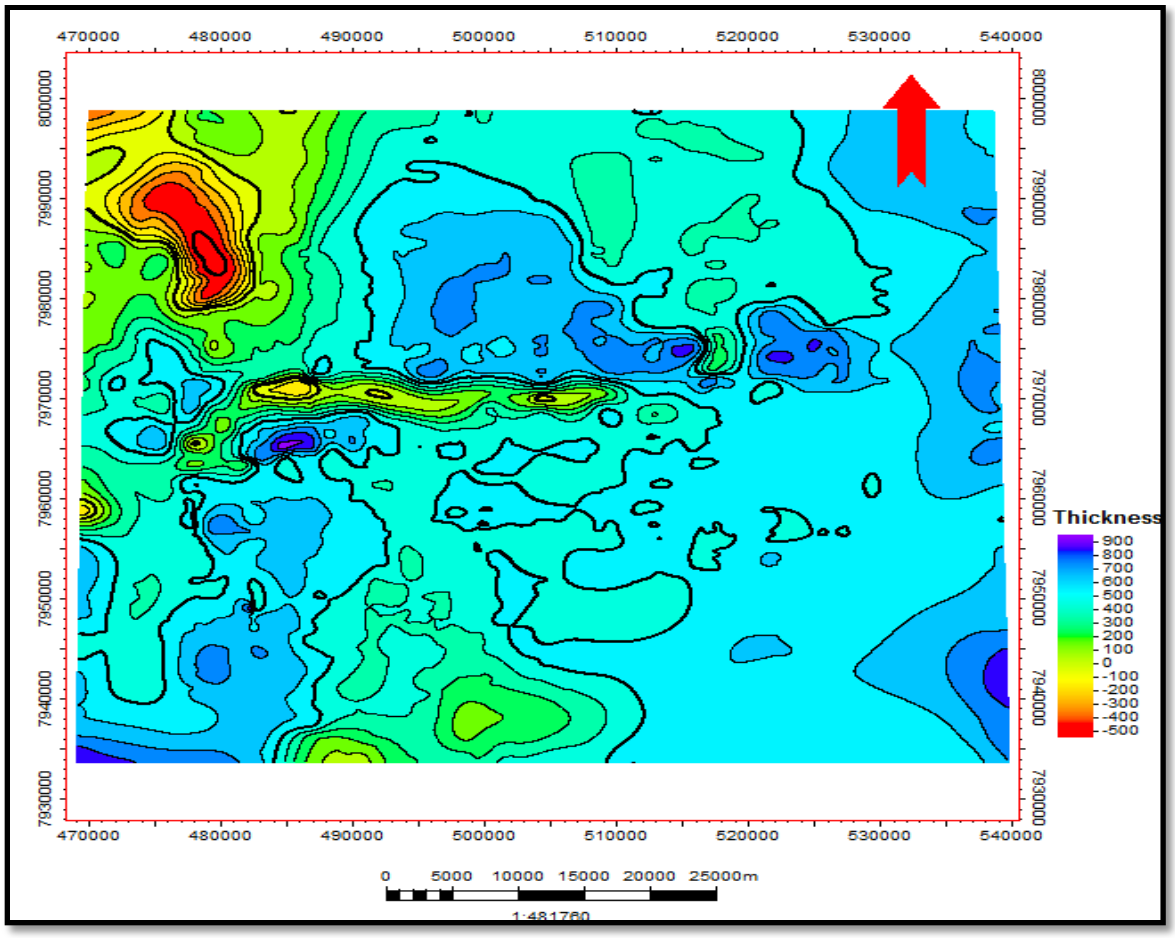

Fig 4.7: Time -thickness map between Intra Carboniferous and Intra Permian reflections

4.5.2 Late Permian to Jurassic

The Triassic to early Jurassic is established as a tectonically quiet period for this region (Gabrielsen et al., 1990) and late Palaeozoic structures controlled the accommodation space in Triassic (Berglund et al., 1986). The Hammerfest basin was a depocentre during early Triassic (Berglund et al., 1986). Time-thickness maps between Mid Permian and Mid Triassic show

thinning towards North West of Loppa High across the Asterias Fault Complex (Fig 4.8). This thinning is attributed to deposition of sediments on a paleo-high (less accommodation space available) lying in the northwest of the present Loppa High (Fig 3.6). Similarly, greater thickness towards eastern side of the study area points to the fact that during this time general tilt of the basin was towards east (Fig 4.8). Absence of growth strata during this period points to lack of rifting in this period (Fig 3.6).

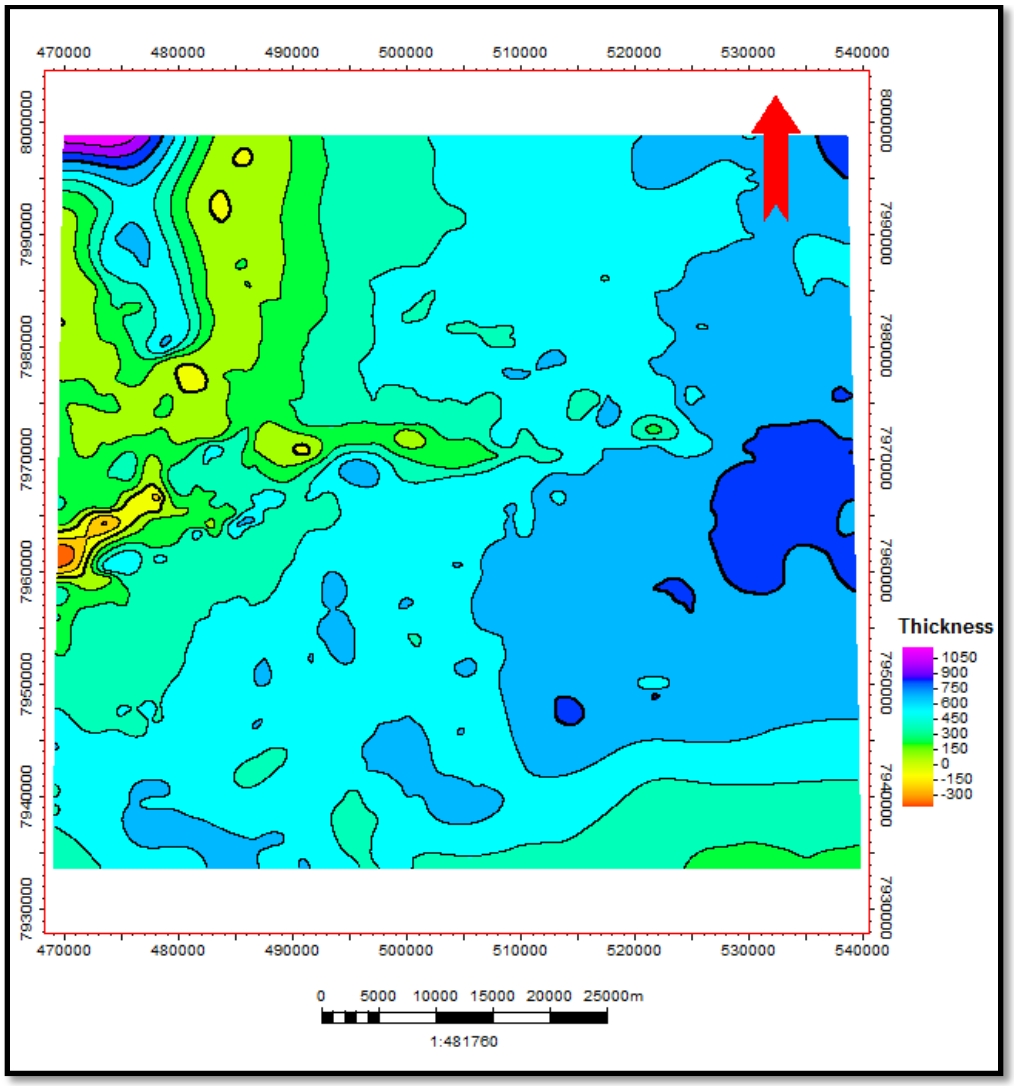

Fig 4.8: Time- thickness map between Intra Permian and Intra Triassic, showing a general thickening trend towards east. Notice the lowest thickness towards north-west of the study area over Loppa High.

4.5.3 Late –Middle Jurassic onset of rifting

Onset of rifting in the southwestern Barents Sea is marked by Late-Middle Jurassic sequence (Faleide et al., 2010). This rifting is coeval with NE Atlantic- Arctic rift system (Faleide et al., 1993). Regional extension accompanied by strike-slip adjustment along the old structure lineaments developing the Bjørnøya, Trømsø and Harstad basins characterizes the Late Jurrasic to earliest Cretaceous structuring in the South Western Barents Sea (Faleide et al., 1993).

Effect of mid late Jurassic rifting phase has been observed based on evidence of growth strata in the hanging wall of the fault complex (Fig 3.8, Fig 3.10). The presence of sedimentary wedges indicates syn-rift sedimentation, suggesting that the fault was active during this period. The Asterias Fault Complex was initiated during Late Jurassic rifting. Additionally, presence of rotated fault blocks within the Jurassic sequence in the Hammerfest Basin augments the idea of Mid-Late Jurassic rifting along with Asterias Fault Complex. Time thickness map reveals thickening of sediments in the north-western side of Hammerfest Basin towards the Asterias Fault Complex which indicates that this part of the study area has experienced more subsidence as compared to other parts (Fig4.9).

4.5.4 Early Cretaceous–Subsidence

Early Cretaceous mark the post-rift stage of late middle Jurassic rifting in the study area.(Fig 4.10)Early Cretaceous onlaps on to the Loppa High in the central compartment (Fig 3.7) indicating uplift and erosion of Loppa High. (Fig.3.6) The limit of Lower Cretaceous is marked on the time structure map. (Fig 3.4.)

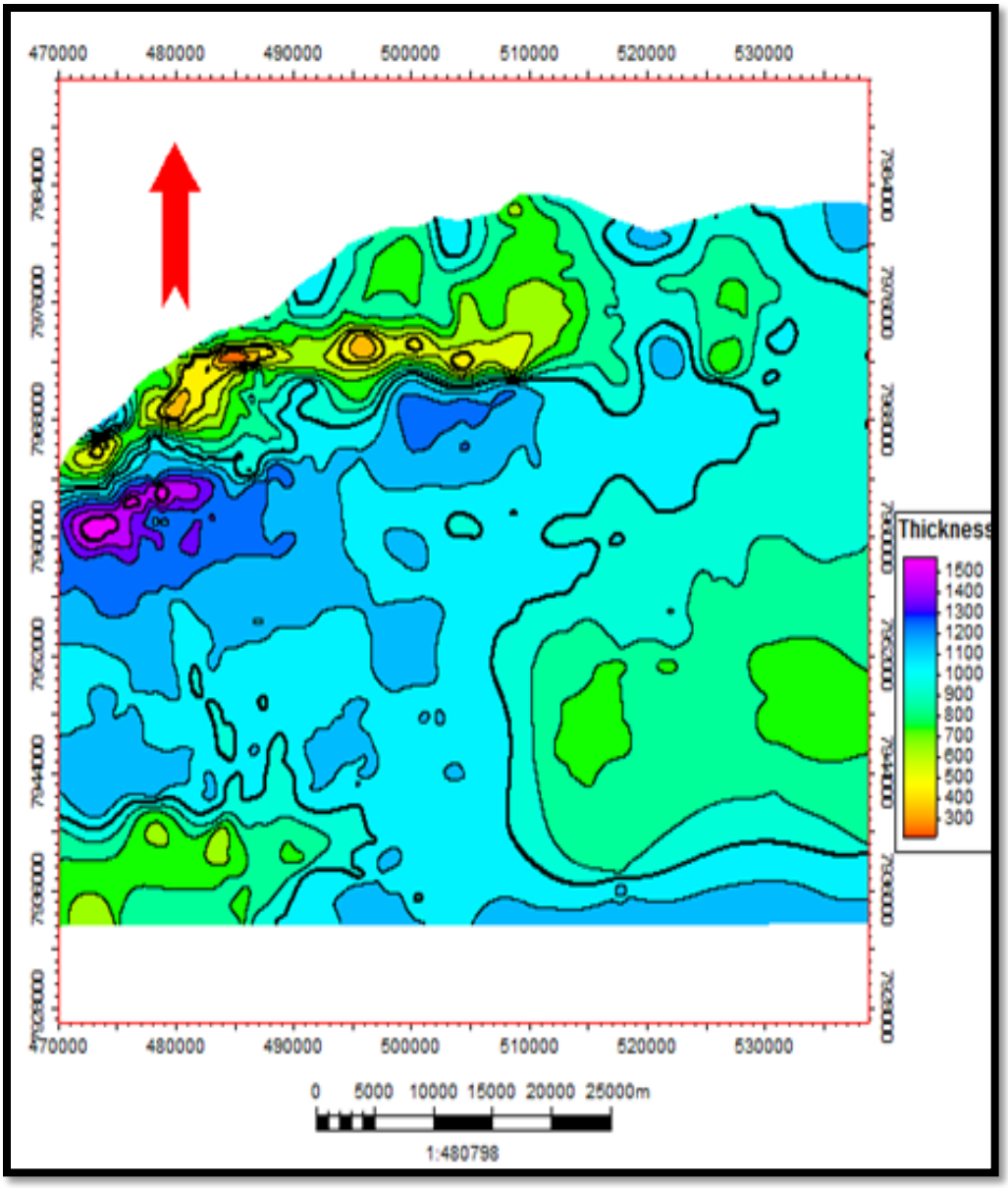

Fig 4.9: Time- thickness map between Intra Triassic and Base Cretaceous reflections. Area of maximum thickness is the north-western part of Hammerfest Basin close to the Asterias Fault Complex.

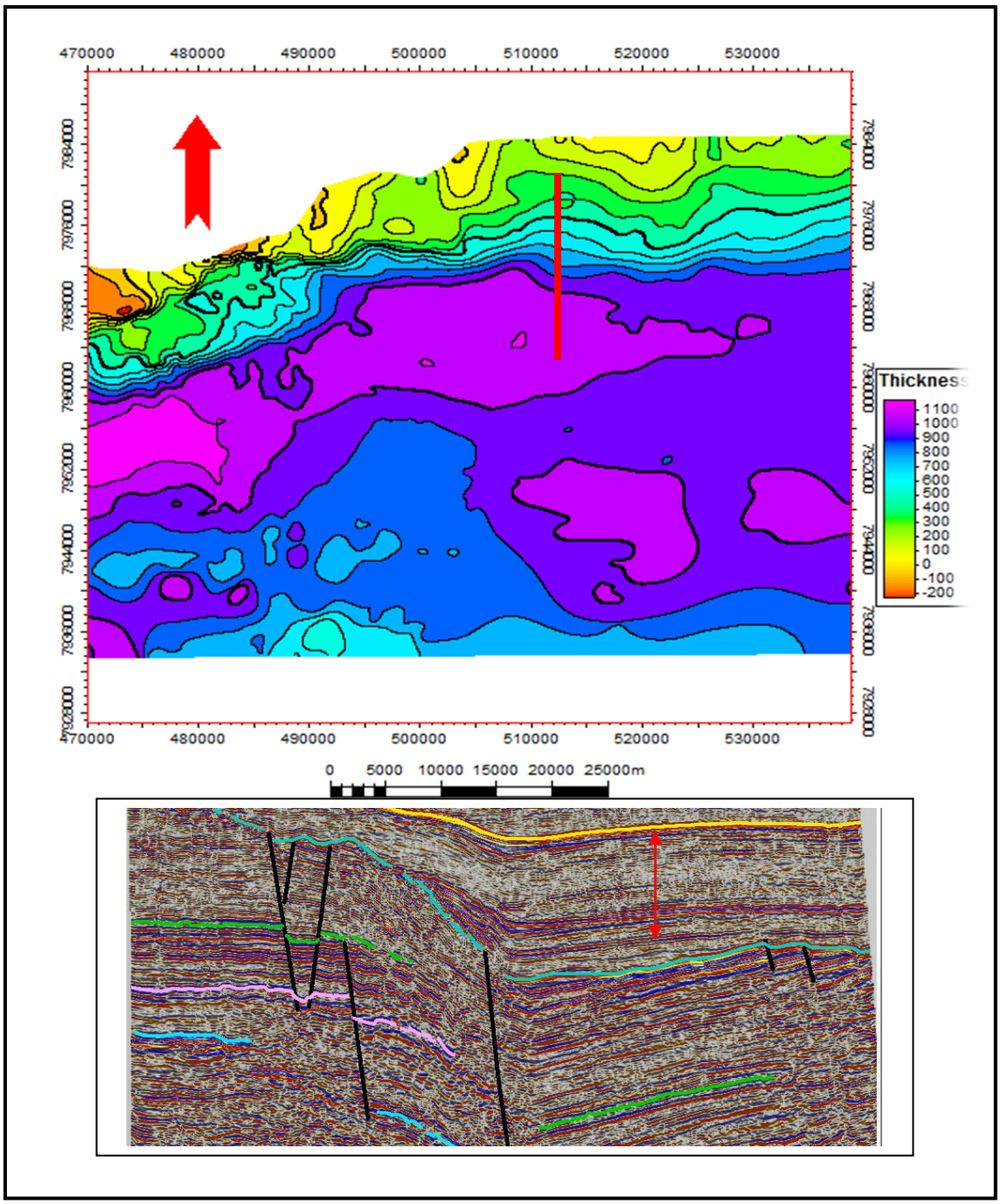

Fig 4.10: Time- thickness map between Base Cretaceous and Base Tertiary reflections. Towards north-western part of the Hammerfest Basin pronounced thinning is observed within the Asterias Fault Complex which significantly increases towards south. Figure 4.9b: Red arrow shows post rift phase of Mid-Late Jurassic rifting. See the colour code in table3.3

4.5.5 Tertiary – Recent

Neogene is represented by a widespread uplift and erosion that is mainly linked with Plio-Pleistocene glaciations (Faleide et al., 1996). Estimates of erosion for the Hammerfest Basin/Loppa High area, range typically between 1000 and 1500 m (Berglund et al., 1986). An unconformity can be recognized in the Late Tertiary sequence of the study area (Fig 3.6, Fig 3.7,3.10). Generalize geological evolution of Asterias fault Complex is given in Fig 4.11

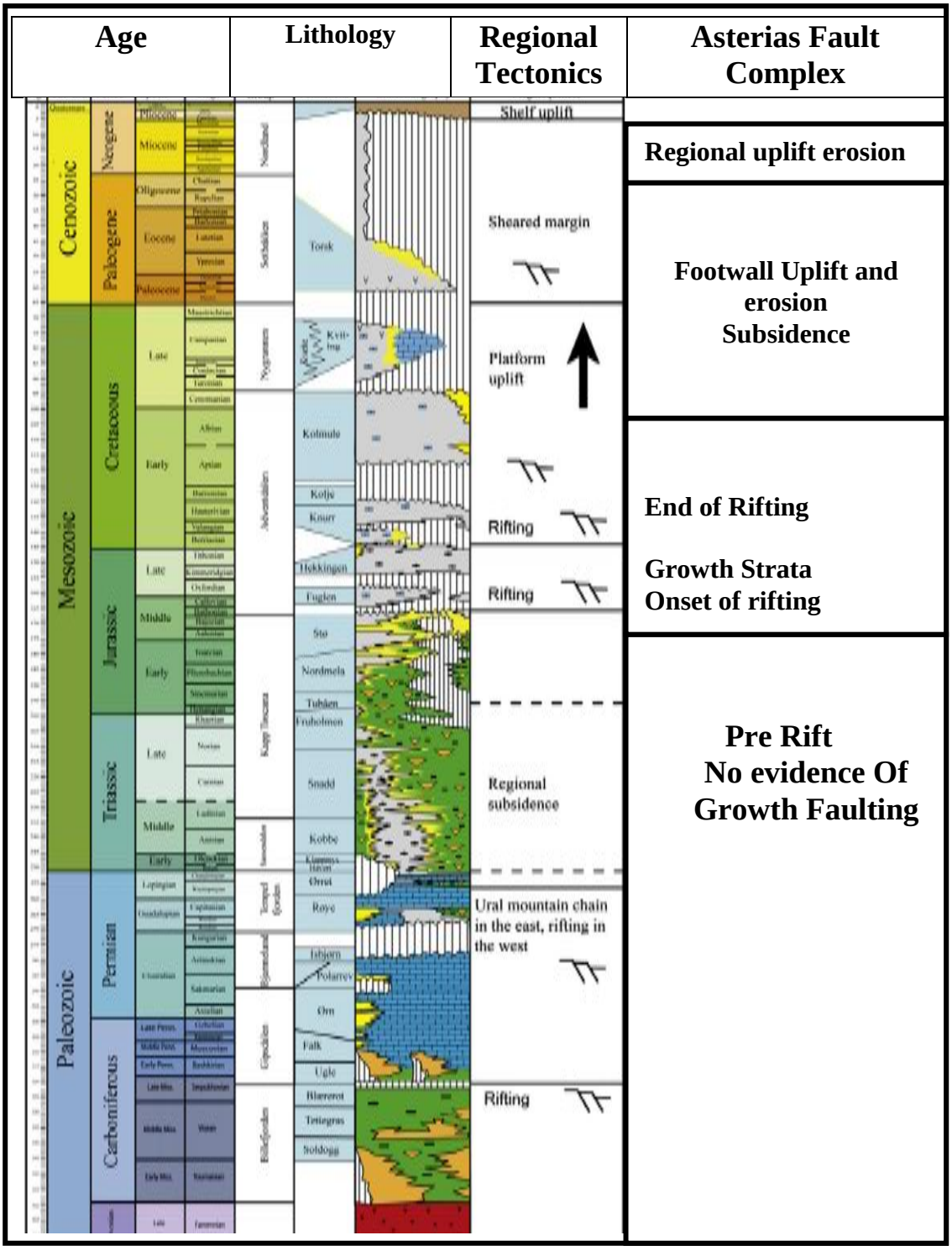

Fig 4.11: Generalized geological evolution of Asterias Fault Complex (modified from Glørstad-Clark et al., 2010)

5 Conclusions

The E-W trending Asterias Fault Complex separating the Hammerfest Basin from the Loppa High is extensional in nature. Three compartments are defined namely the western, the central and the eastern, which exhibit varying degree of deformation (faulting and fault related structuring and vertical displacement along fault) that decreases in intensity from west to east.

The Western compartment has remained the area of much attention in present and previous studies because it offers great challenge in deciphiring the associated complex geometry. The antiformal feature in the hanging wall of main boundary fault was discussed and explained by previous authors and several models were proposed. Rønnevik et al. (1984) relates the formation of this geometry to Late Jurassic wrenching in western and northern Barents Sea, Berglund et al. (1986) introduced the concept of dextral shear and Ziegler et al. (1986) proposed a dextral gravity induced movement responsible for controlling the geometry in this part. After detailed deliberations present study has evolved an altogether new model following the footsteps of Gibbs (1984). The antiformal feature is described as roll-over anticline, formed in the hanging wall ofa listric normal fault. Besides, ramp-flat-ramp geometry is proposed for the western compartment of Asterias Fault Complex based on clear evidence on 3D seismic reflection data.

The ramp-flat geometry prevails in western segment along with associated roll-over anticline and transforms to a downward concave fault in the central segment with little evidence of its related rollover anticline. Fault becomes deep seated and planar in the eastern segment which provides mechanism to form a gentle flexure in the hanging wall.

2D and 3D seismic reflection data lack evidence of growth strata in Carboniferous; therefore the idea of rifting during this period is dismissed in this part of SW Barents Sea. Instead, data reveals that the Asterias Fault Complex and Loppa High were part of same basin and have experienced similar deposition, evident from time thickness maps.

However, there are plenty of evidences to support the Late-Middle Jurassic-Earliest Cretaceous rifting as syn-sedimentry wedges of these periods have been identified. Therefore, an age of Late-Middle Jurassic to Earliest Cretaceous is assigned to the Asterias Fault Complex, prior to which all the sedmentation is attributed to Pre-rift, while younger Early Cretaceous strata is ascribed to be post-rift sedimentation, identified in the Hammerfest Basin.

References

Bally, A. W., 1984. Tectogénèse et sismique réflexion. Bulletin Société Geologique de France, (7)XXIV(2): 279-285.

Barrère, C., Ebbing, J., Gernigon, L. 2008. Offshore prolongation of Caledonian structuresand basement characterisation in the western Barents Sea from geophysical modeling, Geological Survey of Norway. Tectonophysics, 470, 72.

Berglund, L., Augustson, J., Færseth, R., Gjelberg, J. & Ramberg-Moe, H. 1986. The Evolution of the Hammerfest Basin. . In: Habitat of Hydrocarbons on the Norwegian Continental Shelf (Ed. by A. Spencer), 319-338.

Breivik, A. J., Gudlaugsson, S. T. & Faleide, J. I. 1995. Ottar Basin, SW Barents Sea: a major Upper Palaeozoic rift basin containing large volumes of deeply buried salt. Basin Research, 7, 299-312.

Breivik, A. J., Faleide, J.I. & Gudlaugsson, S.T. 1998. Southwestern Barents Sea margin: late Mesozoic sedimentary basins and crustal extension. Tectonphysics, 293, 21-44.

Bugge, T. & Fanavoll, S. 1995: The Svalis Dome, Barents Sea - a geological playground for shallow stratigraphic drilling. First Break 13(6), 237-251.

Cooper, M. A. & Williams, G.D. (Editors), 1989. Inversion Tectonics. Geological Society Special Publications, 44, 335-347.

Dengo, C.A. & Røssland, K.G. 1992. Extensional Tectonic History of the Western Barents Sea. In: Larsen et al. (eds) Structural and Tectonic Modelling and Its Application to Petroleum Geology, NPF Special Publication, 1, 91-107.

Dore, A. G. 1995. Barents Sea Geology, Petroleum Resources and Commercial Potential. ARCTIC, 48, 207–221.

Faliede, J.I., Bjørlykke, K., & Gabrielsen, R.H. ―Geology of the Norwegian Continental Shelf. In Bjørlykke, K. 2010. PetroleumGeoscience: From Sedimentary Environment to Rock Physics, Berlin, Heidelberg, Springeræ-Varalg Berlin Heidelberg. p, 467-501.

Faleide, J. I., Solheim, A., Fiedler, A., Hjelstuen B.O., Andersen, E.S., Vanneste, K. 1996. Late Cenozoic evolution of the western Barents Sea-Svalbard continental margin. Global and Planetary Change, 12, 53-74.

Faleide, J. I., Vågnes Erling And Gudlaugsson, S. T. 1993. Late Mesozoic-Cenozoic evolution of the south-western Barents Sea in a regional rift-shear tectonic setting. Marine and Petroleum Geology, 10, 186-187.

Gabrielsen, R.H. 1984. Long-lived fault zones and their influence on the tectonic development of the southwestern Barents Sea. Journal of the Geological Society London, 141, 651-662.

Gabrielsen, R.H. ―The Structure and Hydrocarbon Traps of Sedimentary Basins. In Bjørlykke, K. 2010. PetroleumGeoscience: From Sedimentary Environment to Rock Physics, Berlin, Heidelberg, Springeræ-Varalg Berlin Heidelberg. p, 299-329.

Gabrielsen, R.H. and Færseth, R.B. 1988. Cretaceous and Tertiary reactivation of master fault zones of the Barents Sea, Norsk Polarinstitutt Rapp. 46, 93–97.

Gabrielsen, R. H., Færseth, R. B. Jensen, L. N. Kalheim, J. E. and Riis F., 1990, Structural elements of the Norwegian continental shelf, Part I: The Barents Sea Region: Norwegian Petroleum Directorate Bulletin, 6, 47.

Gabrielsen, R.H., Grunnaleite, I. & Ottesten, S. 1993. Reactivation of Fault Complexes in the Loppa High Area, Southwestern Barrents Sea. In: Arctic Geology and Petroleum Potential(Editors: T.O. Vorren, E. Bergsager, Ø. A. Dahl-Stamnes, E.Holter, B.Johansen, E. Lie & T.B. Lund), Norwegian Petroleum Society (NPF), 2, 631-641. Amsterdam.

Gibbs, A.D., 1983. Blanced cross section cunstruction from seismic sections in areas of extrnsional tectonics, Journal of Structural Geology, 5, 153-60.

Gibbs, A.D., 1984. Structural evolution of extensional basin margins. Journal of the Geological Society of London. 141, 609-620.

Glørstad-Clark, E., Faleide, J. I., Lundschien, B. A. and Nystuen, J.P. 2010. Triassic seismic sequence stratigraphy and paleogeography of the western Barents Sea area. Marine and Petroleum Geology. . 27, p 1448-1475

Gudlaugsson, S. T., J. I. Faleide, S. E. Johansen, And A. J. Breivik. 1998. Late Palaeozoic structural development of the South-western Barents Sea. Marine and Petroleum Geology, 15, 73-102.

Hamblin, W.K. 1965. Origin of 'reverse drag' on the down thrown side of normal faults. Bulletin of Geological Society of America, 76, 1145-64.

Harding, T. P. 1985. Seismic characteristics and identification of negative flower structures, positive flower structures, and positive structural inversion: Bulletin of American Association of Petroleum Geologists, 69, 582-600.

Harding, T.P. & Lowell, J.D. 1979. Structural styles, their plate tectonic habitats and hydrocarbon traps in petroleum provinces. Bulletin of American Association of Petroleum Geologists, 63, 1016-58.

Jackson, H. R., Faleide., J. I., And Eldholm, O. 1990. Crustal structure of the sheared southwestern Barents Sea continental margin. Marine Geology, 93, 119-146.

Jensen, L.N., & Sørensen, K 1992. Tectonic Framework and Halokinesis of Nordkapp Basin In: Structural and Tectonic Modeling and it Application to Petroleum Geology, R.M Larsen, H. Brekke, B. T. Larsen & E. Talleraas (Eds.) Norwegian Petroleum Society. Special publication, 1, 109-120.

Larsen, G. B. Elvebakk, G. Henriksen, L. B. Kristensen, S.-E. Nilsson, I. Samuelsberg, T. J. Svånå, T. A. Stemmerik, L. and Worsley, D. 2002. Upper Palaeozoic lithostratigraphy of the southern Norwegian Barents Sea.

Rønnevik, H., Bescow, B. & Jacobsen, H.P. 1984. Structural Highs and Basins in the Western Barents Sea. In: *Petroleum Geology of North European Margin* (Ed. by A. M. Spencer), Norwegian Petroleum Society, 19-32. Graham & Trotman, London.

Sund, T., Skarpnes, O., Jensen, L.N. and Larsen, R.M., 1986. Tectonic development and hydrocarbon potential offshore Troms, Northern Norway, Future Petroleum Provinces of the World. In: M.T. Halbouty, Editor, American Association of Petroleum Geologists Memoirs. 40, 615–627.

Worsley, D., Johansen, R. And Kristensen, S. E. 1988. A Lithostratigraphic Scheme for theMesozoic and Cenozoic Succession Offshore Mid and Northern Norway Norwegian Petroleum Directorate Bulletin No.4, 42-65.

Zeiglar, W.H., Doery, R and Scott, J., 1986. Tectonic Habitat of Norwegian Oil and Gas. In: A.M. Spencer et al., (Editors), Habitat of Hydrocarbons on the Norwegian Continental Margin. Norwegian Petroleum Society., Graham and Trotman, London, 339-354.

http://factpages.npd.no/factpages/Default.aspx?culture=en. Last accessed 28th June 2011.

http://www.slb.com/services/software/geo/petrel.aspx Last accessed 28th June 2011.